Advances in Analytic Science 2024, 5(2), 3043.
https://doi.org/10.54517/aas.v5i2.3043

Article

Stochastic dynamics mass spectrometric structural analysis of nucleotides

Bojidarka Ivanova

Institute for Environmental Research, Faculty of Chemistry and Chemical Biology, University of Dortmund, 44221 Dortmund, Germany; b_ivanova@web.de; bojidarka.ivanova@yahoo.com

CITATION

Ivanova B. Stochastic dynamics mass spectrometric structural analysis of nucleotides. Advances in Analytic Science. 2024; 5(2): 3043. https://doi.org/10.54517/aas.v5i2.3043

ARTICLE INFO

Received: 4 November 2024
Accepted: 10 December 2024
Available online: 25 December 2024

Abstract: The paper deals with innovative equations tackling exactly stochastic dynamics mass spectrometric experimental variable intensity of peak per span of scan time. They overcome limitations of classical methods for semi-quantifying analytes developed, so far, and exactly grasp observable variables and their fluctuations; thus, succeeding in determining analytes reliably both quantitatively and 3D structurally via soft ionization mass spectrometry. Given the paper's goal of illustrating their crucial effect on mass spectrometric methodology as an irreplaceable approach to structurally analyse species, this study offers stochastic dynamics-based analysis of nucleotides. The major contribution is providing empirical justification of aspects of structural mass spectrometry analysing uridines and pseudouridines. The virtual identity of fragmentation patterns causes significant analytical challenges. The same is true for methyl-substituted guanosines which are often determined as mixtures. There are used ultra-high resolution electrospray ionization mass spectrometry, high accuracy computational static and molecular dynamics methods, and chemometrics. The study discusses controversial aspects of classical techniques. It illustrates how the innovative equations resolve disputable problems of structural analysis of nucleotides. It supports advanced formulas for achieving superior performances. There are obtained coefficients of linear correlation $|r|$ = 0.9994–0.99923 determining N1-methyl-pseudouridine modified diphosphate compared with 5-methyluridine diphosphate N-acetylglucosamine. There are determined N^2,N^2-dimethylguanosine, uridine, pseudouridine, 5-methyl-uridine, 1-methyl-pseudouridine, 5,6-dihydrothymidine, galactosyl-queuosine, mannosyl-queuosine, adenosine, 2'-O-methyl-5-hydroxymethyl cytidine, uridine triphosphate, thymidine diphosphate N-acetylglucosamine, 5-methyluridine diphosphate N-acetylglucosamine, and 7-methylguanosine-5'-phosphate modified derivative, respectively.

Keywords: stochastic dynamics mass spectrometry; quantum chemistry; nucleotides; 5-methyl-uridine; 1-methyl-pseudouridine; 3D structural analysis

1. Introduction

Uracil is nucleic acid found in RNA—in DNA it is replaced by a 5-methyl derivative (or thymine)—by contrast to nucleic acids determined in both the DNA and RNA [1,2]. Enormous research efforts over decades have been made to comprehensively understand DNA and RNA structures and their replication processes. There is a highlighted connection of RNA point mutation with rare enol-tautomeric uracil forms [2,3]. The RNA modifications play a role in RNA stability and structural folding, translation fidelity, base pairing, cell development and regulation of gene expression. Its modifications are involved in mechanisms of antibiotic resistance and diseases [4]. About 150 modifications in RNA are known [4,5]. The variety ranges from simple modification, which is the most naturally abundant form of nucleotides to modifications including molecular rearrangement [4,6]. Many modifications are homologous to all tRNAs. For instance, there is a TΨC loop containing pseudouridine

(*Ψ*) or the so-called *D* loop, showing dihydrouridine (*D*). Modifications would remain static unless some perturbation of the system such as stress or disease intervened, using RNA-modified nucleotides candidate for clinical analysis in early detection of disease and progression [7]. The molecular structural analysis of (ribo)nucleotides is of outmost importance to in-depth understand not only their biological functions, but also their implementations in fields of medicinal chemistry and toxicology [8]. The chemical substitution of cellular DNA could trigger perturbation in gene expression in addition to induce cell division, or to inhibit apoptosis. Attempts to replicate damaged DNA could cause for errors in cell information.

Oligonucleotide-based therapy using antisense effects is an approach to various diseases [9]. Antisense oligonucleotides joined with target mRNA cause for inhibition effect.

Therefore, the identification and determination of DNA adducts could enhance an in-depth understanding of mechanistic aspects of biochemical reactions associated with carcinogenesis as well as tobacco-related cancers [10].

Due to the prominent role of uracil in cell biology, there are developed 5-substituted uracils with medical applications to oncology or AIDS. Commonly, 5-substituted nucleic bases are templates for constituting antiviral medications [11].

Its derivative 5,6-dihydrouracil is also connected with biological processes. There are transfer loops in RNAs, antitumor, adreno-blocking, or antiretroviral activity [1]. The crucial step, amongst others in the prebiotic formation of cell information which is carried out via DNA and RNA biopolymers is enzyme-free nucleic acid polymerization reactions utilizing cyclic phosphates or phosphoroimidazolides [12]. Thus, low molecular weight (LMW) analytes as ribonucleotides, desoxy-ribonucleotides, amino and fatty acids, and more, are essential components in the organisms [13].

The same is valid for adenosine triphosphate (ATP) and adenosine, which are also implemented into vital cellular biological functions [14,15]. They are co-substrates in enzymatic processes, cell energy production, and extracellular signalling. Extracellular nucleotides are frequently metabolized at the cell surface. The ATP metabolizes to adenosine diphosphate (ADP), adenosine monophosphate (AMP) and, adenosine [14].

There is significant interest in in-depth studying various tautomeric forms of purine and pyrimidine bases as well as their derivatives, due basically to not only their biological importance associated with mispairing by rare tautomers but also to develop of unnatural chemically substituted bases that could extend the genetic alphabet and could find a broad spectrum of application to pharmacy and medicine.

To detail molecular 3D conformations, electronic structure, and energetics of purine and pyrimidine bases and their derivatives; also, their transient species such as cation-radicals is of utmost importance for understanding driving forces in cellular processes involving DNA and RNA. There is looked at mechanistic aspects of biochemical reactions involving radicals and charge transfer effects. The radicals play a primary role in the processes of radiation DNA damage [16]. The thermodynamics shed light on the driving forces of biological processes of the discussed compounds [17].

Further: the protein glycosylation process which is an abundant post-translational modification, amongst other in vivo biochemical reactions plays important roles in a large number of modulation reactions of macromolecular conformation and stability. Its dysregulation is connected with diseases [18–21]. The glucose is used as an energy source in vivo via a glycolytic pathway. It is utilized as a carbon sources for metabolites including nucleotide carbohydrates (CBs) such as substituted uridine 5'-diphospho-N-acetylglucosamine (UDP-GlcNAc) [18].

The monosaccharides are activated *in vivo* by nucleotides through mono- or diphosphate; thus, forming CBs-nucleotides used as glycosylation donors [22]. There are nine human CBs-nucleotides, i.e., UDP-D-Glc, UDP-D-GlcA, UDP-D-GlcNAc, UDP-D-Gal, UDP-D-GalNAc, GDP-L-Fuc, GDPD-Man, UDP-D-Xyl, and CMP-Neu5Ac, respectively.

The nucleotide CBs are used in *Golgi* apparatus. They are added to glycans on proteins. The UDP-GlcNAc is the substrate of GlcNAc-transferases. It is also used to modify O-GlcNAc intracellular proteins [18]. The UDP-GlcNAc is the final analyte involved in the hexosamine biosynthetic pathway [23]. It is a key cytoplasmic amino nucleotide CBs and essential precursor in processes producing different cell biomolecules not only peptidoglycans, but also lipopolysaccharides, chitin, enterobacterial antigens, glycosaminoglycans, glycosylphosphatidylinositol anchors, and more [24].

Due to its significant role in N-or O-glycosylation reactions *in vivo*, enormous effort has been made in designing analogs of UDP-GlcNAc capable of affecting on process of protein *O*-glycosylation by blocking enzyme O-GlcNAc transferase.

Therefore, quantitative and structural analyses of nucleoside modifications in RNA or the so-called *epitranscriptomics* is a crucial step for associating these biologically active molecules with biochemical functions and disease [25–28].

For purposes of molecular structural analysis of species, the analytical practice has used methods for determining base DNA or RNA sequences *via* combinations of enzymatic approaches, chromatography, and radioactive tracer techniques [29–31]. Methodological developments in the field highlight thin layer chromatography and high-performance liquid chromatography coupled with UV-spectrophotometry as methods for an early attempts to quantify such analytes [27], but ultraviolet visible (UV)-detection shows low sensitivities. It mainly determines highly abundant analyte modifications.

Furthermore, there is chiefly semi-quantitative analysis and a lack of quantifying multiple analytes occurs. The indirect and direct next generation sequencing techniques and mass spectrometry (MS) have been proven as powerful tools for identifying analyte modifications. The former tools are high throughput ones.

However, there are required sample pretreatments to recognize sites of macromolecular modification. There is challenge in the distinguishing analyte signal from noise during its mapping.

Hyphenated methods such as liquid chromatography coupled with tandem mass spectrometry are methods of choice for identifying, quantifying, and structurally analyzing sites RNA sequence due to superior method performances. Non-substituted oligodeoxynucleotides could be determined at least qualitatively or semi-quantitatively by means of MS methods at trace concentration levels [29]. The MS

contributes crucially to study mononucleotides, nucleobases, and nucleotides as well as their oligomers and biologically active polymers in their own right [32].

Furthermore, an important research issue is associated with proton accepting capability of nucleosides, nucleobases, and nucleotides in addition to their hydrogen-bond interactions as homo and hetero-base pairs, which frequently involved (doubly) charge and proton transfer effects. They are ubiquitous processes in chemistry and biology [1]. The reactions are, perhaps among most important biochemical pathways of the life itself.

MS methods such as soft ionization approaches to electrospray (ESI) and matrix-assisted laser desorption tools allowing for facile production of large analyte ions in gas phase also contribute crucially to determine protomers, particularly, highlighting that they are characterized by complex multi-centered proton accepting capability and tautomerism [33]. The tautomers have been regarded as inseparable in solution [34].

Nevertheless, uracil has well-studied dominant tautomers. They are different forms coexisting in a solution [2]. A comprehensive analysis by Molina et al. [35] of tautomers, protomers, and cation-radicals has highlighted that a coupled MS instrumental scheme to UV photo fragmentation spectroscopy yields important photodynamic data on protomers of biopolymers and their monomeric sub-units, detailing electronic structure and energetics of cation-radicals of uracil and thymine. Their low-stability and short lifetime challenge MS and UV-electronic spectroscopic analyses.

In the case of 5-methyl-uracil, there is observed a rare enol-tautomer co-existing with its two rotamers [35]. Due to these reasons, the current study, details on tautomers, protomers, and rotamers of the analytes.

Owing to its significant biological activity there have been made enormous effort to study the properties of protomers of uracil and its tautomers of protomers via MS methods, as well [36–44]. For studying RNA, MS approaches are hyphenated with methods for analyte separation such as chromatography or capillary electrophoresis [4]. There is often a level analysis consisting of identifying RNA modifications after a total hydrolysis of the sample. The identifications are carried out via mapped on RNA sequence after digestions to obtain oligonucleotides.

The oligonucleotide MS analysis uses two operation modes—tandem MS/MS and multiple reaction monitoring one—which allows for fast and easy data-interpretation including analyte quantification. Despite, the latter approach requires pre-established data on modified and non-modified analytes.

If a modification is not accurately predicted, then it should not be detected. Gosset-Erard et al. [4] have stated that no software is yet available for untargeted determining of RNA modifications from classical data-dependent MS/MS experimental variables. Long and tedious data-interpretation is manually performed. The analysis of isomers is carried out manually. There are complicated dimensions of MS analysis consisting of theoretical and practical tasks. The latter dimension implicated data-processing of all MS variables of ions, while the former dimension treats fundamental level of theoretical models of exact MS analysis which emerged as response to the fact that isomers of oligonucleotides show often subtle variation of MS data on m/z and intensity of ions. By beginning such analysis one should account not only for MS peaks of analyte, but also data on its isotopomers. Frequently, the latter

peaks show low abundance due to low analyte concentration. Thus, there can be provided ambiguous performances lacking reliability due to fluctuation of MS peaks of isotopomers. The MS study of fate of UDP-GlcNAc utilizes $^{13}C_6$-glucose and $^{13}C_2$-glucosamine and isotopomers analysis [18,45,46]. There is observed complex MS pattern of isotopomers due to ^{13}C-labeled isotopic ions. The MS peaks are assigned to: m/z 606 $[M–H]^-$, 607 (+1) $[^{13}C_1$-$[M–H]^-]$, 608 (+2) $[^{13}C_2$-$[M–H]^-]$, and 611 (+5) $[^{13}C_5$-ribose] in negative MS polarity. The intensity ratio of MS peaks at m/z 606, 607, and 608, using natural isotope distribution shows 1:0.20:0.055 [18]. The latter isotopomer peak often cannot be determined reliably by routine methods for data-processing of variables. The analyte could also participate into reactions of rearrangement causing for migrating phosphate-N-acetylglucosamine moiety to 3' terminus of ribose; thus, complicating experimental MS pattern [23]. Due to these reasons, multiple reaction monitoring MS analysis of CBs-nucleotides yields to r^2 = 0.994–0.998 [47].

Stable isotope tracing of analytes is powerful approach to delineate metabolic pathways. It produces reliable analyte assigning and their quantification via stable isotope tracer MS studies. They focus on distinct analytes or biological pathways [45,46,48–51]. There is a rather lack of comprehensive metabolite coverage analysis *via* the latter technique, due to limitation of known appropriate tools to analyze complex isotope MS pattern of raw data [45,46].

Nonetheless, for purposes of bioinformatics looking at fast and easy data-interpretation there have been developed innovative user-friendly search engines [4,5] comparing absolute intensity data on MS/MS variables with database containing mass spectra of standard samples in order to identify modifications. However, the effectiveness is at about 70 %. Both employment in automated tools and manual MS data interpretation fails to determine dihydrouridine [4]. The analysis of 5-methyluridine (m^5U) and Ψshows effectiveness 50 % depending on sample. The score of determining of Ψ is 34.39 % out of 100 % studying peaks at m/z 245.0754, 155.04527, 179.04479, and 209.05485. The uridine (*U*) shows ion at m/z 245.0754, as well.

Although, a rather lack of strict boundary among bioinformatics' methods and kinetic or thermodynamics ones treating MS phenomena question of reliability of approaches arises for their application to MS variables of oligonucleotides in biological samples.

Mostly, the most stable protomers of tautomers correspond to enol-structures of the discussed analytes. The keto-groups are converted to OH-ones by proton bonding and transfer from neighboring NH groups. The Cooks et al. [52,53] kinetic method and thermodynamics ones [54–57] have reliably determined protonation properties of uracils [1]. Davalos-Prado et al. [1] have comprehensively determined methylated uracils and their protomers via an extended kinetic method based on Cook's kinetic one. It considers entropy effects on dissociation reactions of heterodimeric ions via MS approaches. Cooks et al. and De Pauw et al. [54–58] systematically have developed ESI-MS based protocols for determining stability of protonated dimers of nucleic acids. They are proven approaches to study insight into intrinsic properties of analyte dimers [58]. The methodology involves survival yield method [54–57].

The same can be said for electron ionization MS-based analysis of nucleic acid derivatives which is underlined powerful tool to determine tautomeric equilibria [2].

Post-transcriptional modification in biological processes has been in-depth studied via liquid chromatography platforms and MS instrumentation; thus, resulting in enhanced identification, characterization, and quantification of nucleosides [5]. The highlights are on tandem MS/MS technique determining analyte molecular structure [59–62]. It allows for differentiating among positional isomers; if any. The approach has been applied by Jiang et al. [5] to determine urinary nucleosides. Kuskovsky et al. [5] have analyzed deoxyribonucleotides in fibroblasts via stable isotope labeling technique. Bao et al. [5] have determine nucleoside level in plasma, as well. Limbach et al. [5] have developed automated identification algorithm for MS based determination of chemically modified nucleosides. Quantification of CB-containing nucleotides via ESI-MS shows r^2 = 0.931–0.997 [62]. Analysis of Ψ in RNA has resulted to regression coefficient r^2 = 0.991–0.946 [63].

However, theoretical methods of bioinformatics, thermodynamics, or kinetics ones used to mass spectrometry, so far, are incapable of keeping distinction of reliability straight. The results, so far pose a question of increasing in performances and exact analyte determining via innovative developments of models for data-processing of MS variables.

Besides, experimental MS methods and analytical instrumentation of electronic spectroscopy the theoretical computational methods contribute crucially to (i) understand in-depth biochemical reactions involving nucleosides, nucleobases, and nucleotides; (ii) determine their 3D molecular and electronic structures; (iii) study the structural dynamics of complex processes involving nucleobases; and (iv) obtain thermodynamics and molecular properties of neutral species, tautomers, rotamers, protomers, and cation-radicals, respectively [16,64]. In this regard, computational methods allow for an in-depth understanding of (bio)chemical reactions, because of frequently they exhibit complex mechanisms of condensed phase reactions of nucleic acid derivatives involving solvent molecules [64–66]. Brancato et al. have in-depth studied [16] uracil radicals has, showing that solvent water molecules adopt a cluster-like microstructure instead of a first solvation water shell-like solute-solvent intramolecular arrangements [16].

What is left still unacknowledged in the introductory section is novelty of this study dealing with application of stochastic dynamics MS Equations (2)–(4) (see sub-section 2.1, below) to determine 3D structurally oligonucleotides and, perhaps, to say that these formulas by Ivanova [67–71] provide not only exact quantitative analysis of molecules in environmental and foodstuff samples or biological fluids, but also determine exactly 3D molecular and electronic structures of species. The latter task inherently involves analysis of MS variables and theoretical parameters of quantum chemical computations. There is assessed via chemometric methods statistical significance of mutual linear relation of parameters of Equations (2) and (3).

This study first applies Equations (2)–(4) to determine nucleotides and their derivatives showing a large number of isomers, tautomers, protomers, subtle electronic effects, and significant capability of intramolecular rearrangement, respectively. These properties and processes make their unambiguous MS structural analysis particularly challenging analytical task; furthermore, determining them in mixture. It

is illustrated, how Equations (2)–(4) could be of crucial help in finding highly precise and accurate solution of this problem; thus, achieving excellent method performances.

2. Experimental

2.1. Experimental mass spectrometric method

The sub-section deals with the innovative stochastic dynamics model formulas, as aforementioned.

$$D_{SD}^{tot} = \sum_i^n D_{SD}^i = \sum_i^n 1.3194.10^{-17} \times A^i \times \frac{\overline{I_i^2} - (\overline{I_i})^2}{(I_i - \overline{I_i})^2} \quad (1)$$

$$D_{SD}^{",tot} = \sum_i^n D_{SD}^{",i} = \sum_i^n 2.6388.10^{-17} \times \left(\overline{I_i^2} - (\overline{I_i})^2\right) \quad (2)$$

$$D_{QC} = \frac{\prod_{i=1}^{3N} \nu_i^0}{\prod_{i=1}^{3N-1} \nu_i^S} \times e^{-\frac{\Delta H^{\neq}}{R \times T}} \quad (3)$$

$$I_{\mathrm{SD}}^{\mathrm{Theor}} \approx \left(2.6388.10^{-17} \times D_{\mathrm{QC}}\right)^{1/2} \quad (4)$$

Detail on mutual deriving of Equation (2) from Equation (1) together with approximations used to write Equation (4) from Equation (2) could be found [67–71]. The same is valid to Arrhenius's Equation (3).

Briefly, the equations connect among measurable variables intensity ('I') of MS peak, molecular properties, 3D geometry parameters, and electronic structures of species; thus, allowing to identify and quantify analytes. The analysis is performed per short span of scan time; thus, tackling precisely fluctuations of variables. The fluctuation refers to vary randomly a parameter from its average value over time.

The analysis is performed per short span of scan time. The formulas are applied to any span of scan time of measurement.

Equation (1) contains statistical parameter ,A^i'. It is obtained by means of SineSqr curve fitting of experimental function $(I-|<I>)^2 = f(t)$. It determines temporal distribution of intensity *per* any i^{th} span of scan time. There is obtained error conurbation to A_i-parameter, however. In overcoming the drawback, there is approximated $A^i \equiv 2.<(I-<I>)^2>$; thus, writing Equation (2). It is an exact stochastic dynamics formula for quantitative MS analysis, yielding to $|r| = 1$ [67–71].

The 3D molecular structural analysis is performed *via* equation (2), however, complementary with Arrhenius's Equation (3). The $\nu_i^{(o)}$ and $\nu_i^{(s)}$ represent ionic vibration modes of MS species in ground (GS) and transition (TS) states, while $\Delta H^{\#}$ denotes difference in energetics of same ions in TSs and GSs. The T and R mean temperature, respectively, ideal gas constant. Methods for inferential statistics assess statistical significance of linear relationship $D"_{SD}=f(D_{QC})$.

Equation (4) is derived from equation (2), as well. It predicts highly accurately mass spectrum of molecules approximating $<I^2> > <I>^2$ and $D"_{SD} \sim D_{QC}$. The parameter I_{SD}^{Theor} is theoretical intensity data on MS peaks of q^{th} ion in certain conditions. It does not account for fluctuations of variables. They are unable to be predicted, theoretically.

Equation (4), so far, produces excellent performances $|r|$=0.99922–0.99 [67–71].

2.2. Materials and methods

The study utilizes experimental raw data on MS measurements [72]. There has been used a LTQ Orbitrap XL (Thermo Fisher Inc.) instrument. **Table S1** summarizes experimental conditions of measurements. There are processed data on phage T4 and phage SPO1 nucleosides, where the latter results are from file ORB59709.raw while T4 data are taken from file ORB59710.

2.3. Theory/computations

The GAUSSIAN 98, 09; Dalton2011 and Gamess-US [73–76] program packages were utilized for computing via ab initio and density functional theory molecular species. There were used B3PW91, M062X, and ωB97X-D methods. The Bernys' algorithm determines ground state of ions. The stationary points of potential energy surfaces were determined *via* vibration harmonic analysis. It is proven when there is a lack of imaginary frequency of second-derivative matrix. There were used cc-pVDZ and 6-31++G(2d,2p) basis sets together with quasi-relativistic effective core pseudo potentials from Stuttgart-Dresden(-Bonn) (SDD, SDDAll) [70,71]. The molecular dynamics (MD) computations were carried out by ab initio Born–Oppenheimner (BO) method for M062X functional and SDD or cc-pvDZ basis sets. There were not considered periodic boundary conditions. The molecular mechanics (MM) Allinger's MM2 force field was also utilized [77,78]. The low order torsion terms are accounted for higher priority rather than van der Waals interactions. The method's accuracy is 1.5 kJ.mol^{-1} of diamante or 5.71.10^{-4} a.u. The computations involve crystallographic data on pseudouridine, as well [79].

2.4. Chemometrics

There is used software R4Cal Open Office STATISTICs for Windows 7. The statistical significance was evaluated by *t*-test. Model fit was determined upon by *F*-test. Analysis of variance (ANOVA) tests were used. The nonlinear fitting of MS data was performed *via* searching Levenberg-Marquardt algorithm [80–85]. Together with ANOVA test, there are used nonparameteric two sample Kolmogorov–Smirnov [86], Wilcoxon–Mann–Whitney [87], and Mood's mediantests [88], as well. ProteoWizard 3.0.11565.0 (2017), mMass 5.0.0, Xcalibur 2.0.7 (Thermo Fischer Scientific Inc.) and AMDIS 2.71 (2012) software were used.

3. Results and discussion

3.1. Chromatographic data

Figures S1–S3 depict chromatographic data on ORB59709 and ORB59710. The patterns are not significantly statistically different (**Table S2**). Despite, there shall be discussed some characteristics low intensive chromatographic peaks corresponding to markedly different analyte mass spectra, together with common chromatographic peaks of the samples.

The chromatographic peaks at retention time (RT) = 13.37 and 13.92 mins correspond to abundance MS peaks having Δ (m/z) spacing of 22 (**Figure S4**). They belong to analyte sodium adducts which are frequently stabilized in MS spectra of

nucleosides. The collision induced dissociation (CID)-MS/MS spectrum of MS peak at m/z 244 of ORB59710 yields to product ion at m/z 244 (RT = 13.95 min). It further produces species at m/z 208 and 180 assigned to N^2, N^2-dimethylguanosine (**Figure S5** [89].) The CID-MS/MS of m/z 245.19 and RT=14.23 mins show ions at m/z 246, 226, 207, 179, and 159 typically observed in pseudouridine [5,32] (**Figures S6** and **S7**.)

A low-intensive chromatographic peak at RT = 1.82 min of ORB59709 shows low abundance MS peaks at m/z 581, 561, and 541 of sodium adducts together with MS peaks at m/z 281 and 223. Same characteristic species can be found in mass spectra of galactosyl-queuosine (GalQ) or mannosyl-queuosine (ManQ) [4,90–92].

The CID-MS/MS spectrum of GalQ cation of protomer produces abundance MS peak at m/z 165 (**Figure S8**.) It is assigned to mixtures of m^1G, m^2G, and m^7G isomers [4,6]. It is determined only in sample ORB59709. There is a lack of chromatographic peak at RT = 1.8 min of sample ORB59710. The chromatographic peak at RT = 2.47 min of ORB59709 which lacks of ORB59710 as well as is assigned to adenosine. There is observed abundance MS peak at m/z 136 (**Figure S9**) [4,93]. The typical only for ORB59710 peak at RT = 1.70 min is assigned to 2'-O-methyl-5-hydroxymethylcytidine (hm^5Cm). The data agree with Gosset-Erard et al. work [4]. There are characteristic ions at m/z 286, 142, and 124 (**Figure S10**.)

The peak at RT = 1.17 min of ORB59709 produces MS data on **Figure S11**. Peak at RT = 1.17 min of ORB59709 shows mass spectrum depicted in **Figure S12**. **Figure S13** shows MS spectrum characteristics of 5,6-dihydrouridine triphosphate.

3.2. Mass spectrometric data on nucleotides

3.2.1. Mass spectrometric fragmentation patterns

Before to proceed to apply Equations (2) and (3) to determine 3D molecular structures of nucleotides there is an important issue that this sub-section should address. The species consist of two structural sub-units, i.e., a CBs fragment and nucleic acid which are mutually covalently bonded. There is cleavage of N-glycosidic bond in uridine—a process which can be achieved relatively easily in ESI-MS conditions [94].

Despite, this is not the case of pseudouridine. The N-glycoside bond does not show easy cleavage.

Despite, CBs product ions is formed mainly *via* removal of OH-radical when there is employed in electron impact MS measurements [95]. In presence of phosphate ester bond in substituted nucleosides mechanism of N-glycoside bond cleavage can be complicated due to single or double-strand breaks of phosphate ester bond. It could be implicated in a number of chemical transformations and modifications of nucleobases or CBs moiety. The latter processes; if any, however, could contribute to DNA or RNA mutations [65,95].

Further: When there is N-glycosidic bond hydrolysis of 5-carboxylcytosine, then there is mechanisms of N-glycosidic bond cleavage involving (i) excitation of nucleic acid; or (ii) a stepwise mechanism of intramolecular rearrangement and subsequent C–N glycoside bond cleavage [65]. There is intermediate of hydrogen bond interacting analyte and solvent water molecule, as well. The effect of N^3-protonation of the base

on acidic properties of N^1-centre or presence of 5-COOH substituents is highlighted as important factor, amongst other causing for different chemical reactivity of the bases. Depending on 5-substituent type there can be stabilized additional tautomers or zwitterions as has been detailed on 5-COOH substituted thymine [65].

The MS spectrum of analyte at RT = 2.12 min of ORB59710 shows low abundance MS peaks at m/z 290.09 and 268.10. There is abundance peak at m/z 252.11. The CID-MS/MS data on the latter peak show product ions at m/z 136.06 and 252.11 or 136.06 and 253.11 which belong to standard spectrum of adenosine monophosphate [14,59]. The MS peaks at m/z 290.09 and 268.10 are assigned to sodium adduct of AMP and its protomer, while product ion at m/z 136 is assigned to protonated adenine.

The MS spectrum of ADP and ATP show additional MS peak at m/z 158.92437 [14]. The ATP also exhibits peak at m/z 176.935. It can be assigned to dimers of diphosphate residues. It also reveals MS peak at m/z 408.01. ATP is characterized by low abundance MS peak at m/z 505.9880, as well [14].

The CID-MS/MS spectrum of ψ at m/z 245.0770 shows ions at m/z 125.03473, 155.04523, 179.04512, 209.05576, and 228.06889, respectively [5]. Correlative analysis between intensity data on ions of ORB59710 of CID-MS/MS fragmentation of species at m/z 254.2 at m/z 226.18, 206.94, 178.45, 158.44, 125.19, and 109.58 yields to $|r|$ = 0.07266–0.91257 with or without accounting for results from peak at m/z 226. MS data on ψ also show product ions at m/z 226.8, 208.91, 190.99, 178.93. 154.98, and 124.98 [32]. The analysis between intensity data on these ions with CID-MS/MS ones of samples ORB59710 and ORB59709 of ions at m/z 211.17 (RT = 14.45 min) and 305.08 (RT = 13.65 min) yields to $|r|$ = 0.00975 and $|r|$ = 0.80514 **(Figure S14.)** The analysis of intensity data on ORB59710 and ORB59709 looking at peaks at m/z 208.91, 178.93. 154.98, and 124.98; thus, excluding from results from peaks at m/z 226.8 and 190.99, however, produces $|r|$=0.98053.

The MS spectrum of uridine standard reveals peaks at m/z 113.05, 96.008, 70.029, and 57.034. The m^5U is characterized by ions at m/z 127.057, 110.024, 84.044, 71.6, and 54.03 [96]. Correlative analysis between CID-MS/MS peaks of m^5U at m/z 127.05, 110.024, 84.044, 71.68, and 57.03 [96] and data on ORB59710 yields to |r| = 0.34361–0.99718 with or without accounting for intensity value of peak at m/z 72. The MS ions of standard Ψ and m^5U agree well with results by Giessing et al. [97] and Levola et al. [28]. The electron impact spectrum of pseudouridine-C [98] shows m/z 244 (r.i. 2%; $[M]^+$), 226.0570 (5%; $[(M^+)–H_2O]$), 208.0492 (9%; $[(M^+)–2H_2O]$), 183.0414 (6%), 171.0408 (15%), 154.0379 (16%), 142.0357 (15%), and 141.0289 (100%). CID-MS/MS data on Ψ yield to ions at m/z 209, 125, 191, while m^5U is characterized by fragmentation paths m/z 259 $[M+H]^+ \rightarrow 127 \rightarrow 110 \rightarrow 84$ [99].

Uridine shows ions at: m/z 245 $[M+H]^+ \rightarrow 113 \rightarrow 70 \rightarrow 96$ [97,99]. Depending on experimental conditions of CID-MS/MS measurements there is characteristic MS ion of Ψ at m/z 163. Also, there are observed peaks at m/z 209 and 191 [97]. Derivatives m^5U, m^5C, m^3C, and m^3U produce similar fragmentation patterns: m/z 127, 110, 82, 54 (m^5U); 126, 111, 101, 85, 72, 57 (m^5C); 126, 109, 95, 83, 69 (m^3U), and 127, 109, 96, 68 (m^3U), respectively [97].

A question of further complication of MS based 3D structural analysis of CBs-nucleosides follows looking at data on RT = 15.38 min (ORB59709) and 15.53 min

(ORB59710) (**Figures 1, S15** and **S16**) showing abundance MS peaks at m/z 604 and 609 as well as a low abundance one at m/z 607. The former MS ion ca be assigned to 5-methyluridine diphosphate N-acetylglucosamine (dTDP-D-GlcNAc) which is a nucleotide CB-consisting of m^5U structural sub-unit linked to N-acetylglucosamine or to N1-methyl-pseudouridine modified diphosphate (N1-methyl-ψ_{DP}). Despite the fact that (dTDP)-carbohydrate nucleotides are diverse analytes in the nature, amongst others, and are implicated as glycosylation templates of glycosyl-transferases in obtaining various CBs structures in living cells, their synthesis is significantly challenged [100].

The assigned data on MS peak at m/z 604 agree well with results from a comprehensive MS analysis of nucleoside CBs including the later analyte showing abundance MS peak at m/z 604 and ions at m/z 401, 281, and 269 in negative MS polarity [24,101].

There is variation in MS peak intensity of ions at m/z 604, 605, and 606 comparing with results from UDP-GlcNAc. The peak intensity ratio of ions at m/z 606 $[M–H]^-$, 607 (+1) $[^{13}C_1\text{-}[M–H]^-]$ and 608 (+2) $[^{13}C_2\text{-}[M–H]^-]$ is 1:0.20:0.055 (see comprehensive analysis of molecular isotopomers of complete pentose and hexose ^{13}C-labelled UDP-GlcNAc in [18].) The MS peak at m/z 609 is assigned to 7-methylguanosine 5'-phosphate modified derivative studying a set of structurally similar derivatives and standard samples, as well (below.)

The low abundance peak at m/z 607 is assigned to cation-radical $[M]^{+\bullet}$ of UDP-GlcNAc. In positive polarity it shows abundance peak of $[M+H]^+$ protomer at m/z 608 [102]. In negative MS polarity conditions, the analyte is characterized by abundance MS ion at m/z 606 of $[M–H]^-$ [18,47,103]. Both the UDP-GlcNAc and UDP-GalNAc produce identical product CID-MS/MS ions at m/z 606, 384, 281, and 273 in negative MS polarity mode of operation [47].

The abundance MS peak of CID-MS/MS spectra of UDP-GlcNAc at m/z 591 is identified as characteristics for processes of rearrangement [23]. The peaks at m/z 281 and 263 are assigned to ions of phospho-N-acetylglucosamine structural sub-unit [23]. However, peak at m/z 591 is observed in dUDP-GlcNAc, as well [24,101].

The MS peak at 632 is assigned to sodium adduct $[M+Na]^+$ which agrees with data on [24,101,104] showing that UDP-GlcNAc, dUDP-GlcNAc, and dTDP-GlcNAc tend to stabilize alkali metal ion adducts. The MS peak at m/z 646 is assigned to $[M+K]^+$ adduct. Both the K^+- and NH_4^+-, in addition to sodium adducts are typically observed in MS spectra of nucleoside-CBs [21,105–107].

Therefore, when the study comes to problem of structural assignment of ions at m/z 604, 607 and 609, then the stochastic dynamics approach proceeds as follows: It begins by determining $D"_{SD}$ parameters of Equation (2) of all statistically significantly different datasets of experimental variables and further specifying variation of candidate molecules and their fragment patterns; thus, determining D_{QC} data on Equation (3). Due to complexity of molecular objects, an important point, amongst other, to understand the logic of stochastic dynamics MS based structural analysis is that it solves the problem of reliable distinguishing among structurally very similar species by providing a justification of assignment based on chemometrics assessment of relation $D"_{SD} = f(D_{QC})$. The reliability of assignment is further secured via

independent analysis of theoretical MS spectra obtained via Equation (6) and standard MS spectra of same or structurally very similar analytes.

The CID-MS/MS spectrum of peak at m/z 609.36 of ORB59710 (RT = 15.56 min) shows ion at m/z 610.34. It produces fragment ion showing abundance peak at m/z 591 (**Figure 2**) This ion together with species at m/z 281 and 263 could be assigned to dUDP-GlcNAc and its fragmentation peaks corresponding to intramolecular rearranged species [23,24,101]. The MS peak at m/z 610 corresponds to 5,6-dihydro-dUDP-GlcNAc, while peak at 608.36—to protomer of dUDP-GlcNAc. The CID-MS/MS spectrum of ion at m/z 609 (ORB59709) at RT = 15.38 min is depicted in **Figure 3**.

However, the CID-MS/MS spectra of peak at m/z 391.28 of the both the ORB59709 and ORB59710 reveal common ions at m/z 392, 280, 279, 167, and 149, respectively. Their absolute intensity data (**Table 1**) correlate mutually linearly; thus, showing |r| = 0.99972 (**Figure 4**). The absolute intensity data on MS peaks of isotope shape of 607, 608, 609, 610, and 611 correlate linearly with data on standard guanosine-3'-(*β*-^{18}O-diphosphate)-5'-(*β*-^{18}O-phosphate) (*β*-[^{18}O]-GTP) [108] showing |r| = 0.98497.

However, 7-methylguanosine (m^{7}G) shows MS peaks at m/z 298, 166 and 149 [109,110] together with low abundance ions at m/z 142, 124, 107, and 96 depending on experimental conditions [111,112]. Peak at m/z 167 is observed in spectra of guanosine as result from interaction of product ion at m/z 135 with solvent CH_3OH and subsequent loss of NH_3-group [113]. The same mechanism is used to determine peak at m/z 167 of studied, herein, guanosine derivative. The MS pattern agrees well with those ones of a series of substituted derivatives of m^{7}G [114,115].

If MS peak at m/z 392 (**Figure 2**) is assigned to 7-methylguanosine 5'-(1-thiophosphate) ion, then there are a set of ionic models of product ions.

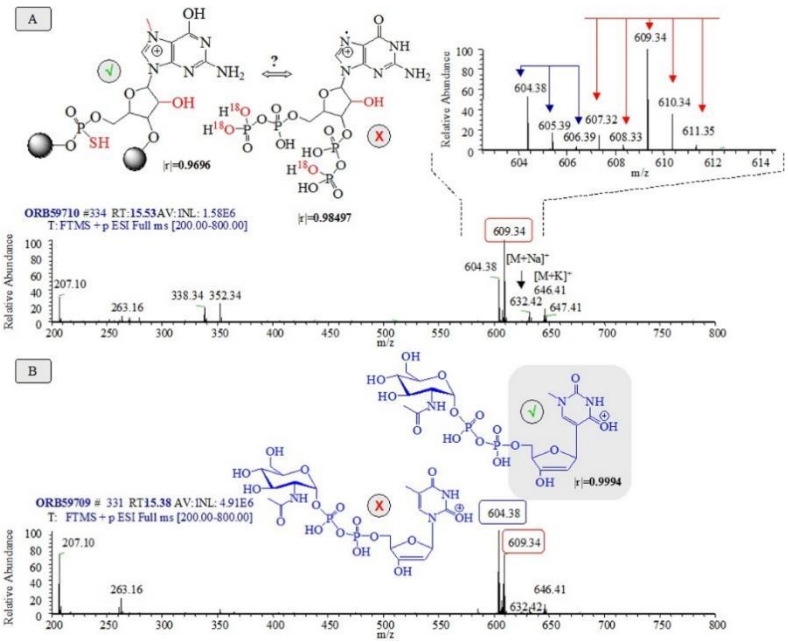

Figure 1. Experimental ESI(+)-MS data on samples ORB59710: **(A)** and ORB59709; **(B)** at RT=15.38 and 15.53 min within m/z 200–800 as well as within

600–620; chemical diagrams of analytes proposed and assigned to ions m/z 604 and 609.

Table 1. CID-MS/MS data on ion at m/z 391 of samples ORB59709 and ORB59710; m/z values; absolute intensity, I [arb.units]; and relative intensity, r.i. [%].

ORB59710			**ORB59709**		
m/z	**I [arb.units]**	**r.i. [%]**	**m/z**	**I [arb.units]**	**r.i. [%]**
149.02	139051.8	100	149.02	153105.4	100
167.03	40142.9	28.87	167.03	41797	27.3
279.16	27548.3	19.81	279.16	25912.4	16.92
280.16	4012.2	2.89	280.16	3590.3	2.34
392.29	10561.5	7.6	392.29	9175	5.99

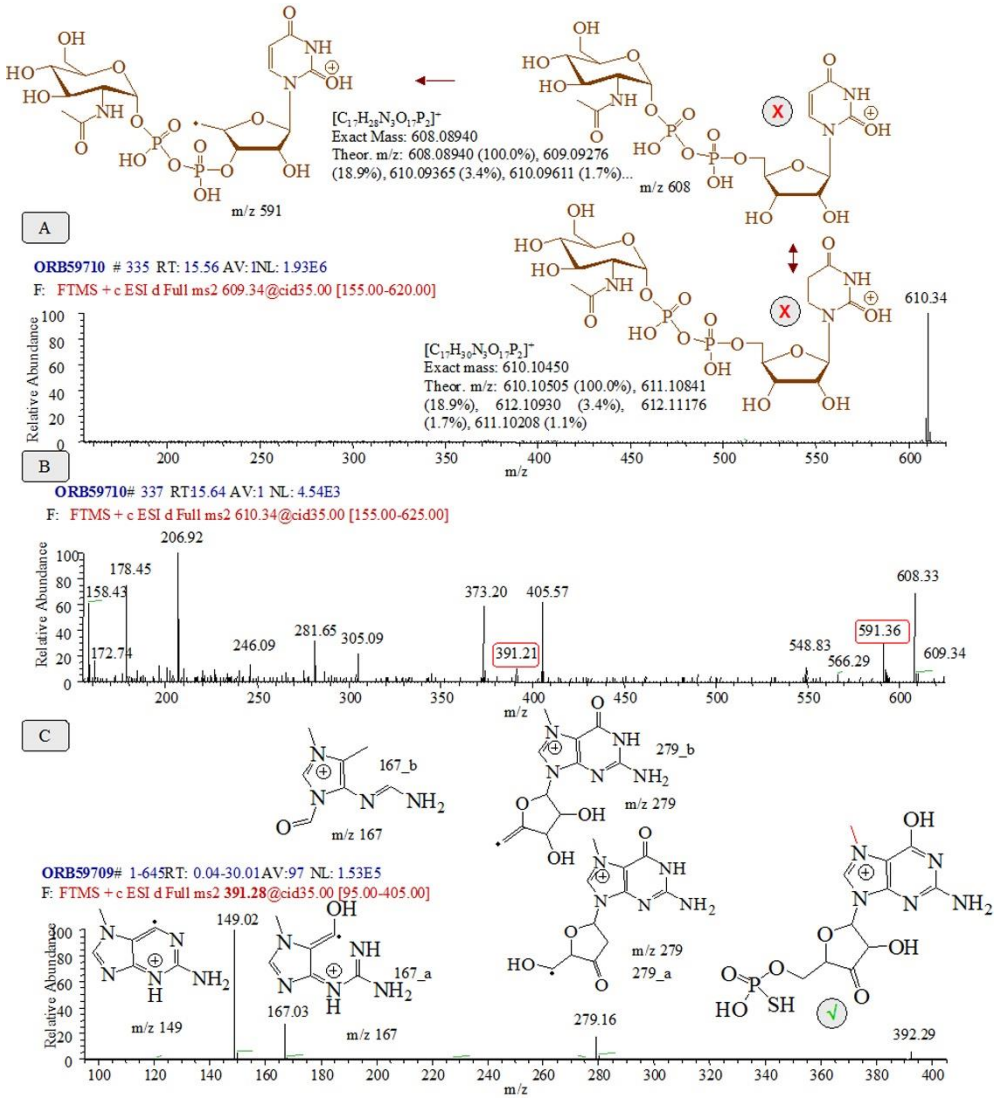

Figure 2. Experimental CID-ESI(+)-MS/MS data on samples ORB59709 and ORB59710 at RT = 15.56: **(A)** 15.64; **(B)** and 0.04–30.01; **(C)** min within m/z 0–600 of ions at m/z 609.34, 610.34, and 391.28; chemical diagrams of proposed analytes and their product ions.

As the introductory section has underlined many of tRNAs homologous contain Ψ or D-loop; thus, showing 1,5-dihydrouridine. If there is taken this view, then there is needed to ask how stochastic dynamics approach should distinguish between $m^1Ψ$- and m^5U-derivatives; if any? In accordance with the innovative approach $D''_{SD}=f(D_{QC})$ relation producing highest |r|—coefficient of ions of $m^1Ψ$- and m^5U-containing species should be assigned to the observable data. **Figures 5, 6, S8**, and **S17–S19** illustrate a statistically representative set of MS ions at m/z 225, 207, 178, 161, 159, 127, 110, and 84, respectively. It allows for a reliable assignment of analytes comparing theoretical and experimental data on various protomers and tautomers of $m^1Ψ$- and m^5U- ions. The MS pea at m/z 179 together with peaks at m/z 213, 196, 161, 101, and 83 are assigned to ions of diphosphate fragment (**Figure S20**). The MS peaks at m/z 211, 210, 193, and 175 belong to ions of substituted CBs-units with phosphates.

The MS peak at m/z 487 (**Figure S13**) is assigned to γ-$^{18}O_2$-uridine-5'-triphosphate (γ-^{18}O-UTP) among the studied series of nucleotides. The results agree well with data on standard stable isotope ^{18}O-labeled derivative [108].

As the preceding sub-section states, the low intensive chromatographic peak at RT = 1.82 min of ORB59709 shows low abundance peaks at m/z 581, 561, and 541, of analyte sodium adducts together with peaks at m/z 281 and 223 which can be found in spectra of GalQ or ManQ [4]. The CID-MS/MS spectrum of the formed cation produces peak at m/z 165. It is frequently assigned to isomeric mixtures of m^1G, m^2G, m^7G [4,6]. The analyte is determined only in ORB59709. There is a lack of chromatographic peak at RT = 1.8 min of ORB59710. The chromatographic peak at RT = 2.47 min of ORB59709 lacks of sample ORB59710. It is assigned to adenosine due to product ion at m/z 136 [4]. The typical only for ORB59710 chromatographic peak at RT = 1.70 min belong to hm^5Cm in accordance with data on same analyte [4]. There are typically observed product ions at m/z 286, 142, and 124.

If there is continued to broaden comparative analysis of analytes of ORB59709 and ORB59710, then there can be seen that at RT = 1.80 min ESI-MS spectrum of the latter sample reveals ions at m/z 178, 167 and 149; thus, studying CID-MS/MS data on ion at m/z 279. The MS spectrum of analyte at RT = 0.62 shows the same ions together with low abundance ones at m/z 392 and 279.16 (**Figure S21**). Concerning similarity of MS pattern of this analyte with the analysis of various substituted methyl-guanosine phosphates [60,61] there is carried out analysis of depicted dimethyl-derivative of guanosine monophosphate (GMP), as well. The MS peaks at m/z 413 and 436 are assigned to mono- and disodium adducts of m^2GMP. The main concern should be: Does analyte at RT = 1.17 min of ORB59709 is β-[^{18}O]-derivative of dimethyl substituted guanosine diphosphate (m^2GDP) or it is β-[^{18}O]-derivative of standard GDP—looking at similarity of fragmentation patterns of **Figures S12** and **S21**?

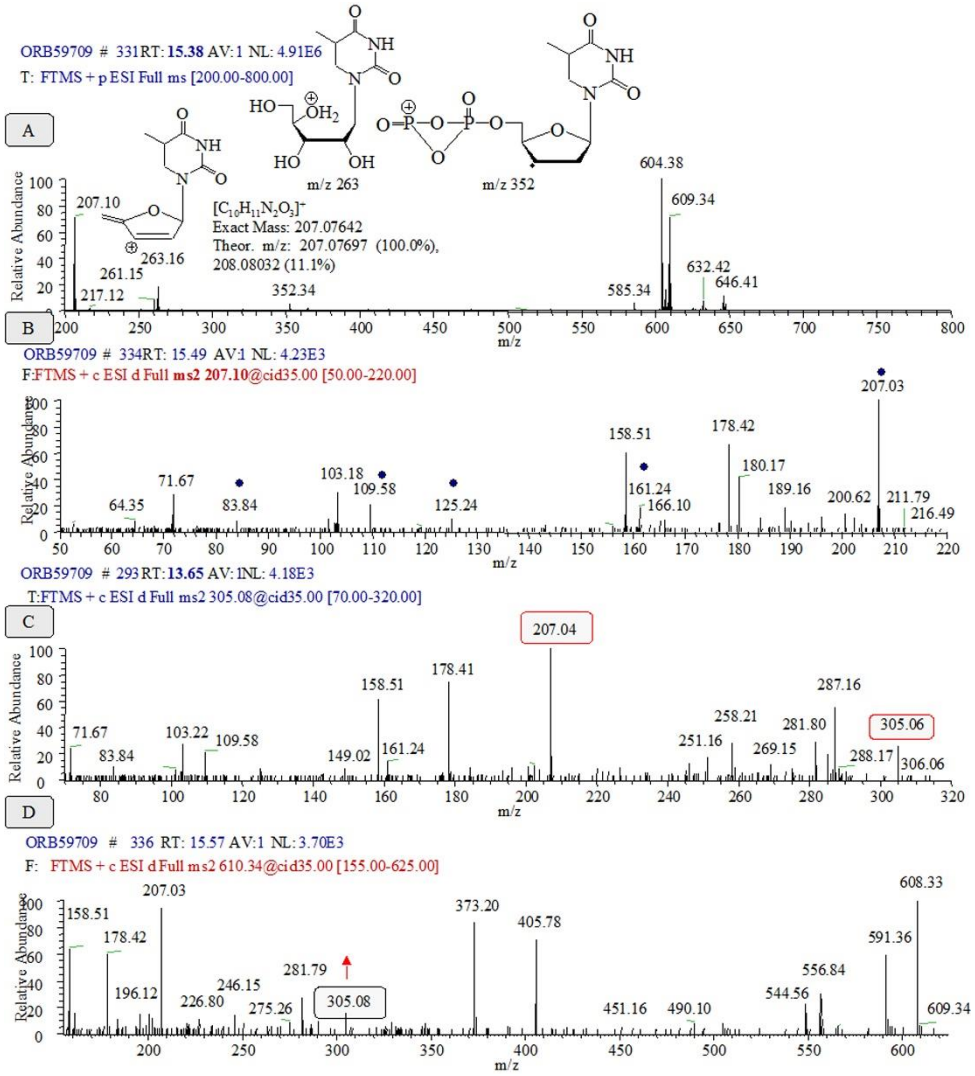

Figure 3. Experimental CID-ESI(+)-MS/MS data on sample ORB59709 at RT=15.38: **(A)** 15.49; **(B)** 13.65; **(C)** and 15.57; **(D)** min within m/z 0–600 of ions at m/z 207.10, 305.08, and 610.34; chemical diagrams of proposed analytes and their product ions.

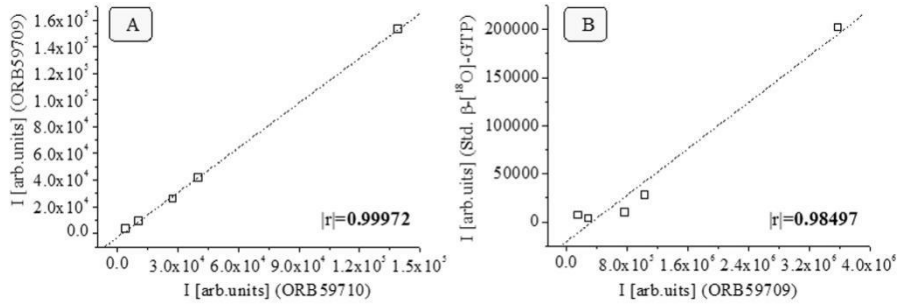

Figure 4. Correlative analysis of absolute intensity (I [arb.uits]) data on CID-MS/MS product ions at m/z 149.02, 167.03, 279.16, 280.16, and 392.29 of ion at m/z 391.28 of samples ORB59709 and ORB59710: **(A)** and ESI-MS isotope peaks of standard β-[^{18}O]-GTP; **(B)** and ESI(+)-MS data on ORB59709 and m/z 607.32, 608.33, 609.34, 610.34, and 611.35.

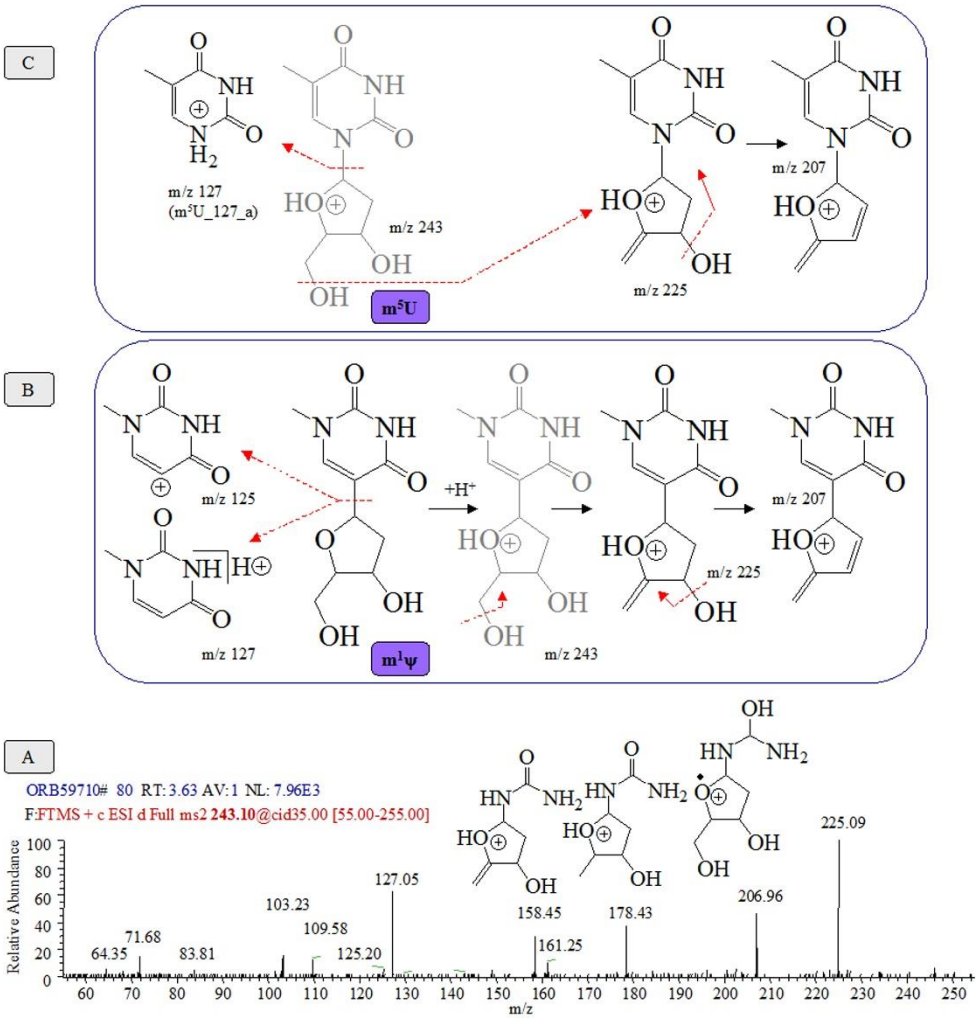

Figure 5. CID-ESI-MS/MS spectrum of analyte of sample ORB59710 at RT = 3.63 min: **(A)** of ion at m/z 243; chemical diagrams of substituted pseudouridine; **(B)** and uridine; **(C)** and their common product ions at m/z 243, 225, 207, and 127, respectively.

3.2.2. Determining of stochastic dynamics mass spectrometric parameters

As could be apparent from what there has been said in introductory section the issue is neither to review capability of equation (2) of exact determining analytes mass spectrometrically nor to detail on theory behind its derivation. The latter matter has been treated at substantial length by Ivanova (2024) [67–71]. The novelty of this study is that it takes question of unambiguous MS-based 3D structural determining of CBs-nucleosides; thus, distinguishing between uridine and pseudouridine containing derivatives via a new, applied for first time approach to process mass spectra of oligonucleotides via Equations (2) and (3). Looking at performances obtained below it seems to be the most accurate approach developed, so far. Following research tasks sketched in [67–71] the $D^{"}_{SD}$ data on Equation (2) are obtained per short span of scan time (**Table S3** and **Figure S22**.) To grasp relation between variable intensity and 3D molecular structure of the species also requires determining of D_{QC} parameters of Equation (3) and I^{Theor}_{SD} ones of Equation (4) (below). The analysis is carried out using datasets of variables of samples ORB59709 and ORB59710.

However, when there are overlapped peaks of the same compounds in the latter samples, then absolute intensity value is taken quantitatively accounting for different amounts of analytes (**Figure S23**). As in the case of chromatographic data shown above, statistical similarity of mean values of m/z variables is evaluated via ANOVA tests (**Table S4**).

3.3. Theoretical data—Correlative analysis among molecular and electronic structures and energetics of ions and determining of Arrhenius's parameter

As the reader has already been noticed that in solving problem of assigning MS peaks of ions to 3D molecular and electronic structures of species via Equation (2) there are favored certain computational tasks. To in-depth understand one the issue, perhaps, one needs to concentrate on concepts of static and MD computations interconnecting between 3D conformations, electronic structures, properties, and energetics of molecules; thus, grasping whole problems of determining most probable 3D molecular structures. There is crucially to answer question "Which 3D molecular conformation belong to MS observable peak?", because of MS data can be studied only knowing of energetics of major MS fragmentation paths of analyte molecules [54,55].

Therefore, the results from this and next sub-sections bridge a gap of knowledge of relations between observable fluctuations of MS variables, particularly, highlighting intensity of peak and analyte 3D molecular conformations and electronic structures.

Despite, the aforementioned almost routinely implemented into the practice algorithms and methods for computing static and MD molecular structures and properties of ions, it represents the most difficult part of the analysis not only because of there is a claim that experimental m/z and intensity parameters of peaks can be directed at 3D molecular structure, but also that the structures and electronic effects can be complex even in cases of small molecules of nucleic acid derivatives.

Yet, there has to be said that the answer to the obvious question "What kind of functional relation do they have?" is that distribution of internal energy of molecules controls their fragmentation paths in unimolecular fragment reactions which are mass spectrometrically observed. The so-called quasi-equilibrium theory in context of MS unimolecular reaction indicates that the analyte dissociation reaction rate in CID-MS/MS experiment depends on molecular internal energy, activation energy of reactions, vibration degree of freedom, and transition state (TS) reaction entropy [56]. There has been established a straightforward correlation between MS intensity of analyte peaks and rate of its CID reactions called survival yield [56,57]. Looking at survival yield relation [56], it is logically to suggest that there is direct functional relation between intensity of MS peak of ion and its energetics.

Since, energetics and vibration modes of molecules are their unique parameters joined to 3D molecular and electronic structure of ions, then, MS intensity values of ions and peaks of an analyte in certain experimental conditions appear unique parameters of 3D molecular structure. A perturbation of measurable variables is closely connected not only with perturbations of conditions of measurements, but also

with perturbation of 3D conformation and electronic structure of molecules. In essence, methods capable of exact processing experimental MS data on, as Equation (2) as well as those ones capable of exact accounting for energetics and vibration properties, as Equation (3), produce highly reliable relation between observable MS phenomena and analyte 3D molecular structure.

Since, function $D^{"}_{SD} = f(D_{QC})$ connects among experimental MS intensity parameters, energetics, and molecular vibrations, *i.e.*, connects between measurable variable intensity and 3D molecular structure this relation written as equation (4) is capable of predicting highly accurately mass spectra of even unknown analytes. It provides relation between 3D electron density map of molecular structure and theoretical intensity I^{Theor}_{SD} parameter.

However, 3D ensemble of atoms called molecule has unique energy parameter and vibration pattern. They are directly connected with MS intensity parameter *via* relation $D^{"}_{SD} = f(D_{QC})$. Equation (2) processes exactly fluctuations of measurable MS data on analytes. It tackles precisely perturbations of 3D molecular conformations and electronic structures. This fact extends significantly the MS capability as a robust method not only for quantitative analysis, but also for highly precise 3D structural analysis when Equation (2) is used complementarily with Arrhenius's Equation (3).

Perhaps, disjunction between known methods connecting between MS spectral and structural similarity as well as Equation (2) is clearly striking; thus, highlighting advantages of the latter approach to molecular structural analysis.

From perspective of theoretical computations and calculation of parameters of Equation (3) there are a number of difficulties to be faces in order to determine precisely 3D molecular geometry and electronic structures as well as energetics of nucleic acid derivatives in spite of structural simplicity of species and the robust capability of computational quantum chemistry as methods and techniques for computing of molecular properties and structures. There is mentioned the major problem of theory that there are a set of analyte tautomers, protomers, rotamers, and radical-cations that produce virtually identical properties. Due to the latter reason computational tasks imply a set of objects of analysis.

Despite, the fact that it might be said that methodology is mere technical, however, it does not really matter. As a matter of fact subtle electronic effects producing two closely distinct electronic structures never really do share same vibrational properties in spite of cases of equal energy parameters or so-called isoenergetic structures. The theoretical analysis needs to be maximum close enough in properties of species in order to produce plausible structural assignment of peaks using relation $D^{"}_{SD} = f(D_{QC})$.

In doing so, there are studied a large number of molecular and electronic structures of species in order to distinguish reliably between ions and to achieve statistically the true assignment of discussed theory and innovative model equations.

Thus, in the case of uracil containing species as has been comprehensively theoretically studied over decades there are eighteen tautomers. Raczynska et al. systematically detail on most stable species of non-substituted uracil [60,116,117].

The so-called *antiaromatic form* (protomer of tautomer $m^5U_{\_207\_T1}$ of ion at m/z 207 in **Figure S19** or ion $m^1\psi_{\_207\_a}$ in **Figure S17**) is considered as most stable [116–120].

The *aromatic form* (ions $m^5U_{\_207\_T5}$ and $m^1\psi^{-207\_d}$) shows increasing in stability with increasing in solvent polarity. High accuracy computations (CASSCF(10,8)/6-31+G**) show that in both the gas-phase and polar solvent there is stable nonaromatic form of uracil. There is also decreasing in the index deviation from aromaticity from 5.256 to 4.998 [118] due to subtle electronic effects or intramolecular rearrangement [121]. These effect, however, cause for significant change of ionic vibrations of species in both the ground state (GS) and TS; thus, producing markedly different D_{QC} parameters.

As there is highlighted above, different electronic effects perturb experimentally observed MS intensity parameters crucially. The electronic effects should be tackled assigning MS patterns of derivatives of nucleic acids.

Further: Problem with this study is that substituted uridine and pseudouridine derivatives produce virtually identical fragment ions at m/z 207, 127, 110, and 84, respectively. The electronic effects of tautomers and rotamers of species should be tackled highly accurately in order to distinguish not only among protomers of tautomers or rotamers; if any, but also between two molecular structural derivatives.

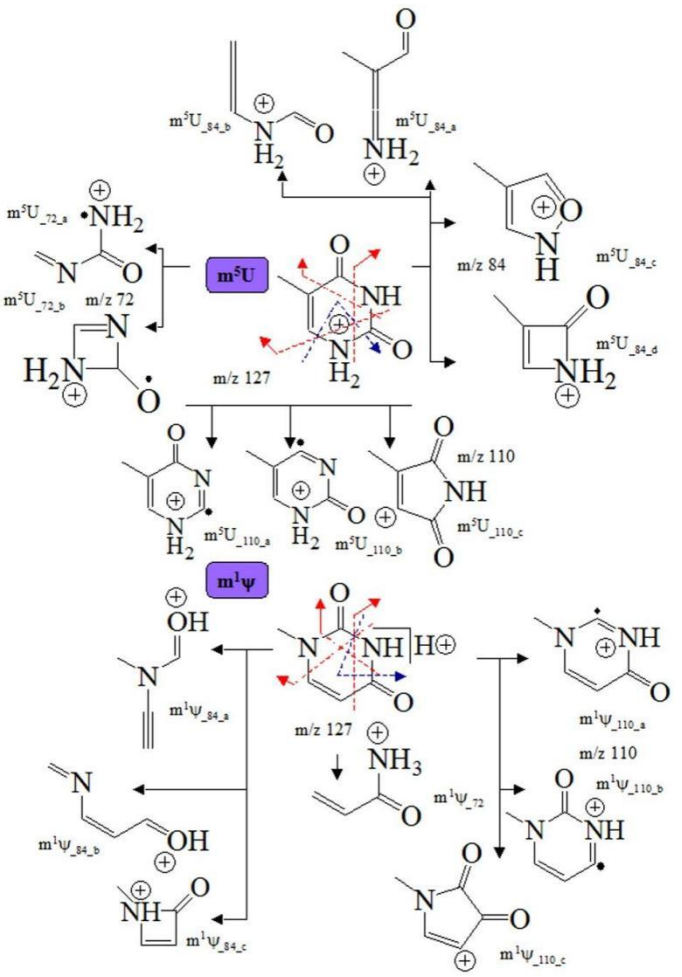

Figure 6. Chemical diagrams of ions of 5-methyl-uracil (5-methyl-1*H*-pyrimidine-2,4-dione) and 1-methyl-uracil (1-methyl-1H-pyrimidine-2,4-dione) at m/z 127, 110, 84, and 72, respectively.

Nevertheless, that the latter statement, perhaps, should a bit complicated research tasks, and, in fact, this is a rather complicated pro-argument favouring Equations (2) and (4), however, the figures already shown illustrate what is meant. The presence of two identical peaks in mass spectrum of mixtures of analytes containing substituted uridine and pseudouridine means that there are two molecules that were not reliably distinguishable even utilizing ultra-high resolution mass spectrometric experiments.

Conversely, within the stochastic dynamics method analytes are highly reliably distinguishable in mixtures assigning observable MS peaks to significantly distinct molecular parameters, despite complexity of their tautomers due to their vibration modes, even in cases when the molecular systems produce isoenergetic ions.

After considering theoretical data on protomers of tautomers and rotamers of ions of m^5U and $m^1\psi$ at m/z 207 and 127 (**Figures S24–S27** and **Table S5**) it seems that there should be said that more stable is species $m^1\psi_{\_207\_a}$ and $m^5U_{\_207\_T1}$ showing C = $O^{2+}H$ protonation position. The former cation is most stable one comparing with the latter ion showing energy difference ΔE^{TOT}=|0.009826| a.u.

Although, it is easy to suppose that the same trend of thermodynamics stability of ions should be observed in other product ions of m^5U and $m^1\psi$ as the latter figure reveals it is difficult to define preliminary the most stable product ion. The results from protomers of tautomers of ion at m/z 127 reveal that most stable is protomer of OH-tautomer of substituted uridine ($m^5U_{\_127\_e}$) comparing with series of $m^1\psi$ ions showing lowest energy of $m^1\psi_{\_127\_a}$. Comparison with tautomers of protomers of these ions should help the reader to see difficulty involved in this research task. If there is asked to identify analytes precisely via MS method then there should be accounted for subtle electronic effects of protomers and tautomers. They are characterized by different vibrational properties.

The properties of species which have been mentioned throughout this and preceding sub-sections include perturbation due to intramolecular rearrangement and proton, respectively, charge transfer effects in addition to effects of protonation and tautomerism. A particular emphasize in this context needs the fact that reactions of intramolecular rearrangements could involve not only nucleic acid bases, but also phosphate subunits [107,122].

Since, there are a set of competitive reactions of phosphates; thus, producing MS peaks at low m/z values, which alter structural analysis of nucleotides they are theoretically considered in this work, as well**.**

Results from ions at m/z 225 and 207 of m^5U as well as m/z 125 and 110 of $m^1\psi$ showing intramolecular rearrangement are illustrated in **Figure 7**, as well.

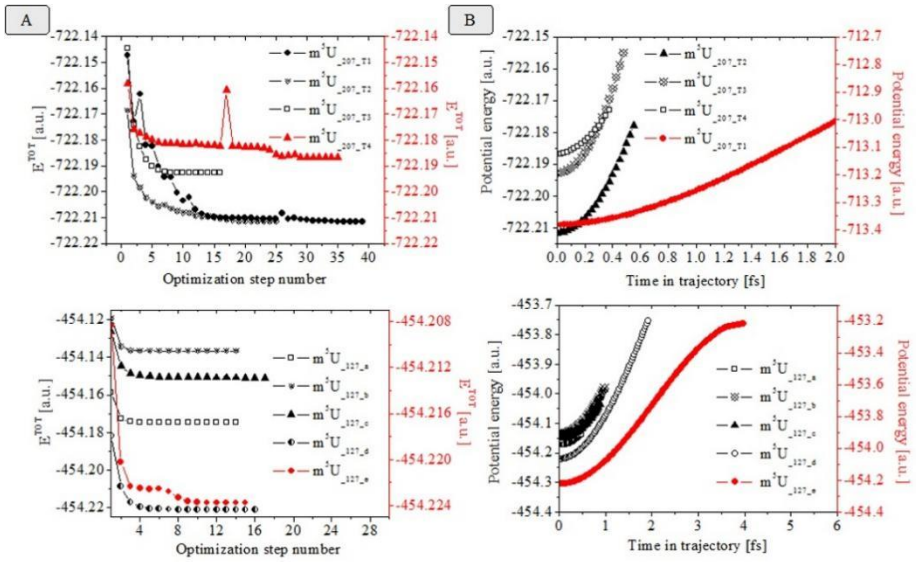

Figure 7. Theoretical M062X/SDD data on various tautomers and protomers of m^5U ions at m/z 207 and 127: Total energy, E^{TOT} [a.u.], with respect to optimization step number: **(A)** Born-Oppenheimer molecular dynamics data; **(B)** Potential energy [a.u.] versus time in trajectory.

Let at this point return to D_{QC} parameter of Equation (3). Looking at results from **Tables S5–S7** there are ionic properties of species which are needed to proceed to calculate D_{QC} parameter of ions depending on their molecular structure and electronic effects. They affect both the energetics and vibration properties. Vibration modes depend on subtle electronic effects. They allow to distinguish reliable protomers of tautomers even studying structurally very similar ions. The later fact is major advantage, among others, of presented approach to 3D structural analysis of analytes, mass spectrometrically.

Since, the paper, so far, has not done much to detail on the issue, then there should be attempted to say something substantial about it at this point.

Looking at experimental MS spectra of nucleotides presented, so far, there has been arguing that different analytes uridine and pseudouridie, among other ones produce virtually identical MS patterns. This fact, forces us to use stable isotope labelling approach to determine analytes as among most reliable method for MS identification and annotation of compounds in biological samples. As results from **Figure 4** reveal there is achieved high statistical parameter of linear correlation $|r| = 0.98497$, which further, is affected weakly in cases of small structural differences of analytes. Therefore, increasing in reliability of analysis needs introduction of independent approach to determine molecular structure which to account precisely for subtle variation of molecular skeleton and electronic effects. The vibrational modes of species as D_{QC} parameters show are such a tool tackling precisely effect of 3D-molecular conformation and electronic structure on intensity parameter of MS observable peak of ion. As can be seen, there is obtained marked difference in D_{QC}-parameters (**Table 2**). The later fact draws attention to how statistical assessment of relation $D^{"}_{SD} = f(D_{QC})$ is capable of determining subtle variations of structure of nucleotides; furthermore, reliably. The statement seeks to defend relative complexity

of calculation tasks of the innovative approach. In favour of this tool there can be noted that next subsection clearly indicates that subtle variations of electronic structures of anaytes, having complex electronic effects are processed with a significant difference in chemometric performances using D_{QC} parameters of various forms. It correlates D_{QC} data with experimental MS ones of Equation (2) of ions of the discussed analytes.

Table 2. The D_{QC} and I^{Theor}_{SD} parameters of Equations (3) and (4) of protomers of tautomers and isomers of parent and product ions of nucleotides observed mass spectrometrically.

m/z	Form	m^5U		m/z	Form	$m^1\psi$	
		D_{QC}	I^{Theor}_{SD}			D_{QC}	I^{Theor}_{SD}
247	$m^5U_{\_247}$	202.8749	$7.3168.10^{-8}$	-	-	-	-
225	$m^5U_{\_225}$	12.3023	$1.8018.10^{-8}$	225	$m^1\psi_{\_225}$	113.4484	$5.4715.10^{-8}$
207	$m^5U_{\_T1}$	156.945	$6.435.10^{-8}$	207	$m^1\psi_{\_207\_a}$	3490.904	$3.035.10^{-7}$
	$m^5U_{\_T2}$	91.2268	$4.9064.10^{-8}$		$m^1\psi_{\_207\_b}$	165.2345	$8.48.10^{-7}$
	$m^5U_{\_T3}$	273.4428	$7.9152.10^{-8}$		$m^1\psi_{\_207\_c}$	160.371	$6.505.10^{-8}$
	$m^5U_{\_T4}$	102.4092	$5.1985.10^{-8}$		$m^1\psi_{\_207\_d}$	127.832	$5.808.10^{-8}$
178	$m^5U_{\_178}$	239.313	$7.9467.10^{-8}$	-	-	-	-
161	$m^5U_{\_161}$	70.4746	$4.3124.10^{-8}$	-	-	-	-
159	$^5U_{\_159}$	31.4547	$2.881.10^{-8}$	-	-	-	-
127	$m^5U_{\_127\_a}$	161.885	$6.522.10^{-8}$	127	$m^1\psi_{\_127\_a}$	406.982	$1.0363.10^{-7}$
	$m^5U_{\_127\_b}$	113.7976	$5.4799.10^{-8}$		$m^1\psi_{\_127\_b}$	199.0407	$7.2473.10^{-8}$
	$m^5U_{\_127\_c}$	18.6705	$2.2196.10^{-8}$		$m^1\psi_{\_127\_c}$	187.4298	$7.02604.10^{-8}$
	$m^5U_{\_127\_d}$	281.2731	$8.61524.10^{-8}$		$m^1\psi_{\_127\_d}$	178.874	$6.8703.10^{-8}$
	$m^5U_{\_127\_e}$	388.7157	$1.0128.10^{-7}$		$m^1\psi_{\_127\_e}$	555.3707	$1.2106.10^{-7}$
125	-	-	-	125	$m^1\psi_{\_125}$	89.2184	$4.8521.10^{-8}$
110	$m^5U_{\_110\_a}$	104.5565	$5.3653.10^{-7}$	110	$m^1\psi_{\_110\_a}$	5547.4226	$3.826.10^{-7}$
	$m^5U_{\_110\_b}$	37.3567	$3.1397.10^{-8}$		$m^1\psi_{\_110\_b}$	1559.1612	$2.0284.10^{-7}$
	$m^5U_{\_110\_c}$	96.8784	$5.056.10^{-8}$		$m^1\psi_{\_110\_c}$	248.5196	$8.098.10^{-8}$
84	$m^5U_{\_84\_c}$	64.3464	$4.1206.10^{-8}$	84	$m^1\psi_{\_84\_a}$	224.5864	$7.6983.10^{-8}$
	$m^5U_{\_84\_d}$	249.169	$8.1086.10^{-8}$		$m^1\psi_{\_84\_b}$	233.061	$7.8422.10^{-8}$
					$m^1\psi_{\_84\_c}$	2321.52	$2.475.10^{-7}$

3.4. Correlative analysis between theoretical and experimental mass spectrometric data

The most important issue that is really to be addressed in this study is statistical significance of linear relation between $D^{"}_{SD}$ and D_{QC} data on Equations (2) and (3) or chemomerics assessment of relation $D^{"}_{SD} = f(D_{QC})$. **Figures 8** and **9** illustrate distinction among protomes of tautomers of uridine and pseudouridine derivatives showing important significance; thus, allowing to assign unambiguous MS peak to 3D ionic structures of analytes.

The cases discussed in reminder of this sub-section raise very important and challenging questions, regarding not only practical application of Equations (2), (3) or (4) to determine reliably derivatives of m^5U and $m^1\psi$ in biological samples, but also

their reliable MS based determination via classical approaches, as well. The MS phenomena of newcomers of analytical instrumentation are still not exhaustively understood. The fact makes essentially amenable to study them via modeling methods. The current study promotes innovative models of both MS methodology and fragmentation processes of nucleotides; furthermore, in mixture, both of which are not readily grasped, so far. The methodological developments of theoretical model formulations are very helpful for grasping the latter issues.

Arguably, it can be done exactly via Equation (2). It only tackles fluctuations of MS data. As the discussed data stand, there is explanation and assignment of MS phenomena of ESI-conditions of MS measurements, which model Equations (2)–(4) do capture exactly from perspective of chemometrics.

Therefore, they produce highly reliable assignment of experimental MS data to 3D molecular structures of species; thus, allowing a detail structural analysis of mixtures of biological samples containing the discussed analytes even studying unknown samples.

Discussing results from this sub-section, there is obtained persuasive chemometrics showing excellent performances. They allow for a moving of a view that soft ionization MS methods are significantly challenged in distinguishing quantitatively among similarly substituted mixtures of m^5U and $m^1\psi$ containing compounds to one that aforementioned MS methods provide unambiguous 3D structural analysis of such analytes even studying biological samples. The last statement guest to most important matter: The irreplaceable capability of MS methods not only for quantifying analytes in biological samples but also for determining them 3D structurally; furthermore, unambiguously when the structural analysis involves Equations (2) and (3) or (4).

The further analysis could be of help in clarifying the latter statement. Due to low signal-to-noise ratio and analyte concentration CID-MS/MS reactions of ion at m/z 266.18 cause for significant fluctuation of both the m/z value and intensity of ions (**Figure 8, Table 3**). ANOVA tests show that variables at m/z 72, 84, 103, 125, 159, 178, 207, and 247 are not statistically significantly different. There is large standard deviation (sd(yEr±)), however (**Table S4**).

The correlative analysis of intensity data on the peaks yields to low |r|- coefficient (**Figure 8B**). In such case; if any, it is not simple identification of analytes *via* classical methods, due to low performances of MS data on standard samples [28].

Returning to Equations (2) and (3) and assessment of relation $D"_{SD} = f(D_{QC})$ the correlation between average intensity data on ions with D_{QC} parameters of ions of m^5U shows $|r| = 0.98831$ (**Figure 8C**). Thus, with the shown statistical significance there are assigned the peaks: m/z 161.2486 ± $3.67.10^{-4}$ ($m^5U_{\_161}$), 178.4396 ± 0.012 ($m^5U_{\_178}$), 206.943 ± 0.017 ($m^5U_{\_T3}$), and 247.052 ± 0.1659 ($m^5U_{\_247,}$) respectively. The parent ion at m/z 266.17 is assigned to sodium adduct of m^5U.

Much the latter point could be carried out by contrasting capability of classical MS methods and innovative stochastic dynamics approach, because of what has been MS observed of 1-methyl-, 2-methyl-, and 7-methyl-guanosine [96] as standard analyte data on, far is applicable to distinguish unambiguously them in mixture via classical methods for data-processing of measurands. Jora et al. [96] have provided a

comprehensive analysis of the analytes showing |r| = 0.91088 of data on common peaks of m^1G and m^2G at peaks at m/z 110, 128, 149, and 167, respectively.

However, correlation of intensity data on common peaks at m/z 110, 149, and 167 of m^1G and m^7G yields to |r| = 0.99998 [96]; thus, lacking of their reliable distinguishing in mixture *via* classical approaches. In the case of sample ORB59709 and CID-MS/MS results from **Figure 2** shown above correlative analysis between observable in this study intensity data and standard one yields to |r| = 0.9696 (**Table 4**, **Figure 9A**). Again, due to significant fluctuations of variables there is obtained large sd(yEr±) value.

Despite, only application to classical methods lacks of distinguishable capability between m^7G and m^1G derivatives. Obviously, novel methodological point needs crucially to be made and it is implementation of relation $D^{"}_{SD} = f(D_{QC})$ of Equations (2) and (3) into structural analysis of nucleotides. It provides not only exact assessment of fluctuations of variable, but also is based on different theoretical methods accounting for 3D molecular structures and electronic effects of analytes. Owing to different fragmentation patterns of m^1G and m^7G there are observed variations in 3D molecular structures and electronic effects of species which are accurately tackled with static and MD methods; thus, producing reliable D_{QC}-parameters (**Table 2**). The links with exact intensity parameters of species is performed with Equation (2). Relation $D^{"}_{SD} = f(D_{QC})$ accounts for exact and real link between MS observable variables and 3D molecular structures of species. This fact brings the paper to results from **Figure 9** showing |r|-data up to 0.99946 when assessing experimental and theoretical parameters of m^7G derivative of CID-MS/MS spectrum of ion at m/z 391 of ORB59709 and ORB59710 shown as **Figure 2** and data on **Table 4**. The analysis of the $D^{"}_{SD}$ data on peaks at m/z 279, 167, and 149 of product ions of CID-MS/MS spectra of cation at m/z 391.18 of samples ORB59709 and ORB59710 yield to |r| = 0.99996 (**Figure 9C**). There is an identical analyte of the samples assigned to the shown derivative of m^7G.

Therefore, application to the latter novel methodological procedure sheds light on, and solves problem of reliable distinguishing of isomers of m^1G and m^7G which is incapable of performing *via* classical methods as shown above.

At this point we are in position to discuss much of what has been already said about capability of relation $D^{"}_{SD} = f(D_{QC})$ of structural determining of nucleotide isomers having virtually identical MS patterns; thus, detailing on a more expanded form the data on **Tables 2, S3, Figures 2** and **9**. We might begin discussion looking for basic principles used to distinguish between 5-methyluridine diphosphate N-acetylglucosamine containing m^5U structural sub-unit and N1-methyl-pseudouridine modified diphosphate. The correlative analysis between theoretical and experimental data on ions at m/z 207, 110, 161, and 84 in the case of dTDP-D-GlcNAc shows |r| = 0.98541–0.97402 (**Figure 9C**). There are assigned peaks to: m/z 207 ($m^5U_{\_207\_T3}$), 161 ($m^5U_{\_161}$), 110 ($m^5U_{\_110\_b}$), and 84 ($m^5U_{\_84\_c}$), respectively.

However, comparative analysis of $D^{"}_{SD}$ and D_{QC} data on N1-methyl-Ψ_{DP} species producing the same MS peaks at m/z 225, 207, 110, and 84 yields to excellent performances (|*r*| = 0.99946–0.99923) (**Figure 9D**). The excellent correlation among D_{QC} parameters with experimental intensity data of peaks looking at most stable 3D

molecular and electronic structures of analytes indicates the following assignment of ions: m/z 225 ($m^1\Psi_{\_225}$), 207 ($m^1\Psi_{\_207\_}$), 225 ($m^1\Psi_{\_225}$), 110 ($m^1\Psi_{\_110\_c}$), and 84 ($m^1\Psi_{\_84\_b}$), respectively. The application of Equation (4) yields to |r| = 0.99459. The analysis of data involving D_{QC} parameter of $m^1\Psi_{\_207\_b}$ shows |r| = 0.99946.

The consideration supposes significant importance for understanding of stochastic dynamics formulas as tools for solving problem of MS based 3D structural analysis of mixtures of derivatives of nucleotides, having common MS fragmentation patterns and virtually identical intensity parameters, due to molecular structural similarity and small variation of chemical substitution.

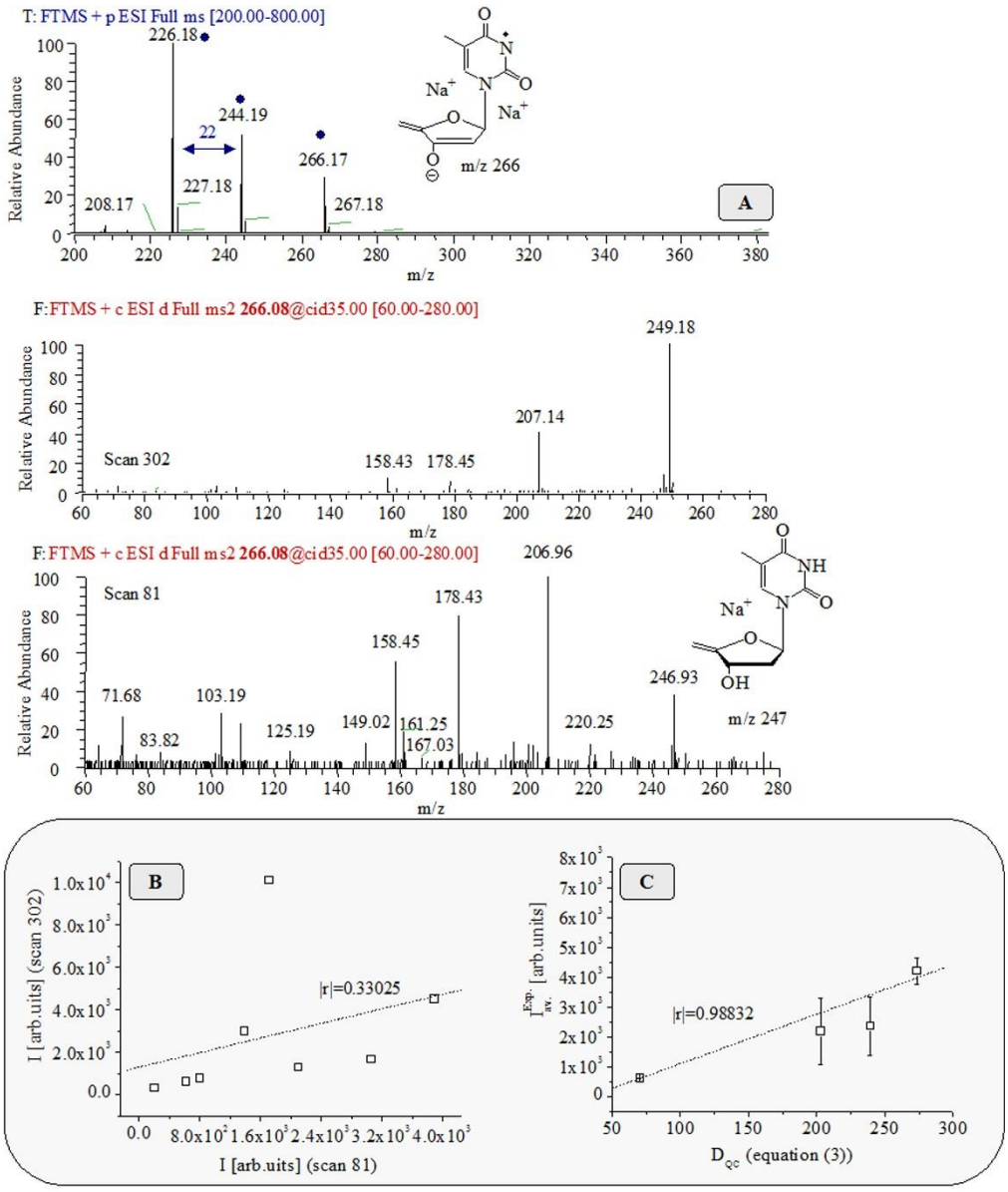

Figure 8. ESI(+)-MS and CID-MS/MS spectra of ORB59710 and cation 266.18 of scans 81 and 302; chemical diagram of analyte: **(A)** linear correlation between absolute intensity data (I [arb.units]) of product ions of spectra of scans 81 and 302 (**Table 3**); **(B)** correlation between average intensity data ($I^{Exp.}{}_{av.}$ [arb.units]) on ions of (A) and D_{QC} parameters of Equation (3) shown in **Table 2; (C)** chemometrics.

Table 3. Experimental CID-MS/MS data on 266.18; m/z and intensity, I [arb.units], of product ions of sample ORB59710 depending on scan number 81 and 302; descriptive statistics.

Scan 81		**Scan 302**		**Average**	
m/z	I	m/z	I	m/z	I
109.57905	802.5627	109.57895	772.11119	$109.579 \pm 7.013.10^{-5}$	787.337 ± 21.5325
125.19485	203.50537	125.17997	315.47021	125.1874 ± 0.01052	259.4878 ± 79.1711
158.45114	2104.63477	158.3969	1287.05685	158.424 ± 0.03836	1695.8458 ± 578.1149
161.24887	620.93299	161.24835	603.81062	$161.2486 \pm 3.67.10^{-4}$	612.372 ± 12.1074
178.43073	3063.09655	178.44841	1660.40706	178.4396 ± 0.01251	2361.752 ± 991.8513
206.95532	3894.12788	206.93114	4510.47776	206.9432 ± 0.0171	4202.303 ± 435.8252
207.00717	1715.30202	207.1353	10114.5289	207.0712 ± 0.0906	5914.916 ± 5939.1503
246.93414	1389.14206	247.16887	2981.23991	247.052 ± 0.16598	2185.191 ± 1125.783
		249.18492	24845.2586		

Table 4. Temporal distribution of observable variables (m/z values and intensity, I [arb.units]) of ORB59709 per span of scan times or scan numbers 29, 36, and 46 of CID-MS/MS data on peak at m/z 391.18 (**Figure 2**); descriptive statistics; $D"_{SD}$ data on Equation (2); average m/z and intensity data.

Scan	**m/z**	**I**	**m/z**	**I**	**m/z**	**I**
29	279.15863	14189.8548	109.5777	762.02816	125.25979	142.02775
36	279.15884	18927.9087	109.57767	844.39166	125.28191	243.69354
46	279.15897	20878.1351	109.57786	719.54583	125.28338	153.94612
Mean	279.15881	-	109.57774	-	125.27503	-
sd(yEr±)	$1.70.10^{-4}$	-	$1.02.10^{-4}$	-	0.01322	-
se(yEr±)	$9.81.10^{-5}$	-	$5.92.10^{-5}$	-	0.00763	-
$\langle I \rangle$	-	17998.6329	-	775.32188	-	179.88914
$\langle I \rangle^2$	-	$3.24.10^{8}$	-	601124.018	-	32360.1027
$\langle I^2 \rangle$	-	$3.32.10^{8}$	-	603810.129	-	34419.277
$\langle I^2 \rangle - \langle I \rangle^2$	-	$7.89.10^{6}$	-	2686.11169	-	2059.17433
$D"_{SD}$	-	$2.08.10^{-10}$	-	$7.09.10^{-14}$	-	$5.43.10^{-14}$
Scan	m/z	I	m/z	I	m/z (av.)	I (av.)
29	149.02307	35768.6888	167.03342	12808.9596	125.2_8	179.89 ± 55.58
36	149.02318	52182.8144	167.03355	19261.5899	109.577_7	775.32 ± 63.48
46	149.02312	163425.369	167.03375	38772.0813	149.02312	83792.3 ± 69450.9
Mean	149.02312	-	167.03357	-	167.03	23614.2 ± 13517.8
sd(yEr±)	$5.36.10^{-5}$	-	$1.69.10^{-4}$	-	-	-
se(yEr±)	$3.09.10^{-5}$	-	$9.74.10^{-5}$	-	-	-
$\langle I \rangle$	-	83792.2908	-	23614.21	-	-
$\langle I \rangle^2$	-	$7.02.10^{9}$	-	$5.58.10^{8}$	-	-
$\langle I^2 \rangle$	-	$1.02.10^{10}$	-	$6.79.10^{8}$	-	-
$\langle I^2 \rangle - \langle I \rangle^2$	-	$3.22.10^{9}$	-	$1.22.10^{8}$	-	-
$D"_{SD}$	-	$8.49.10^{-8}$	-	$3.21.10^{-9}$	-	-

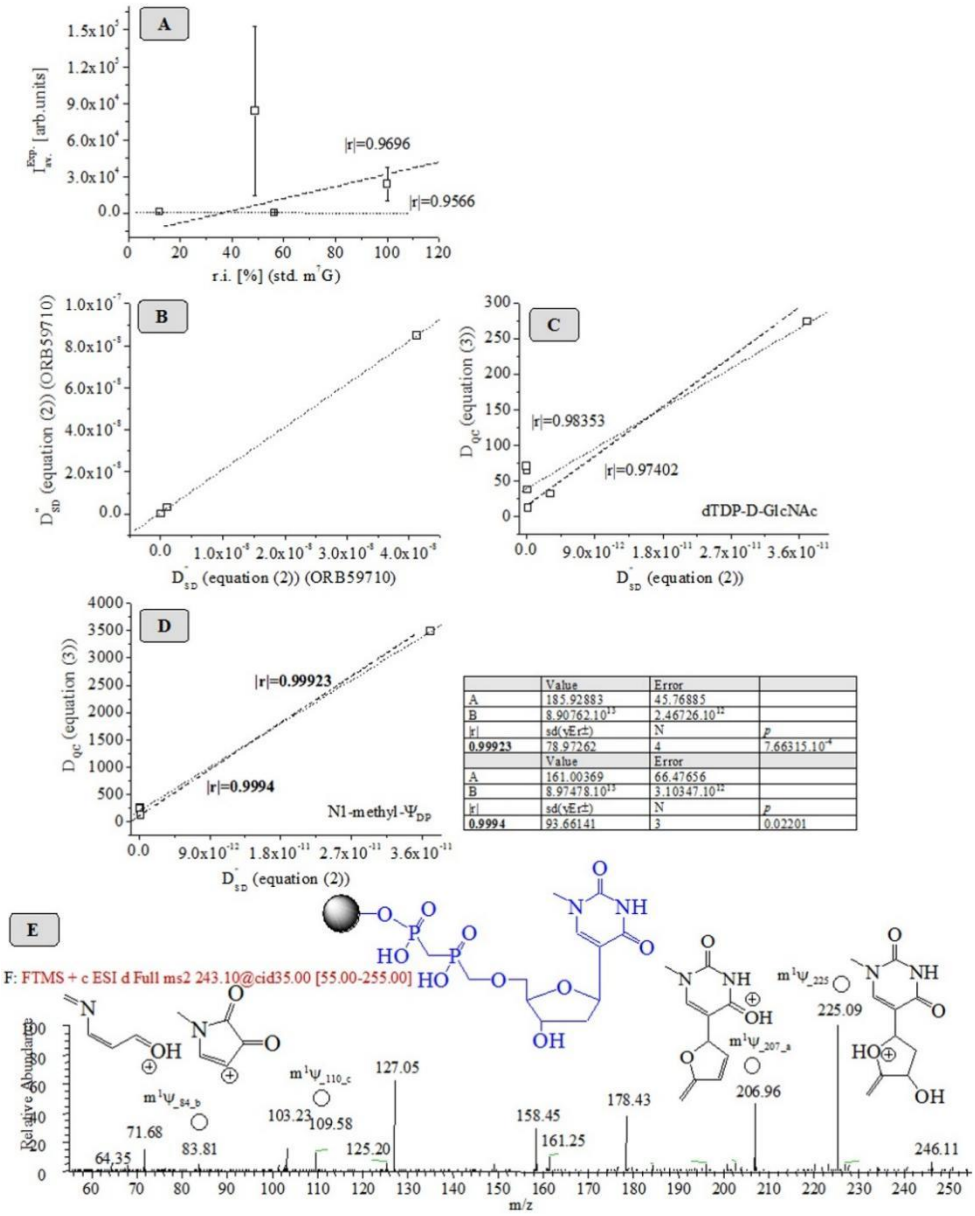

	Value	Error	
A	185.92883	45.76885	
B	$8.90762.10^{13}$	$2.46726.10^{12}$	
|r|	sd(vEr±)	N	P
0.99923	78.97262	4	$7.66315.10^{-4}$
	Value	Error	
A	161.00369	66.47656	
B	$8.97478.10^{13}$	$3.10347.10^{12}$	
|r|	sd(vEr±)	N	P
0.9994	93.66141	3	0.02201

Figure 9. Correlative analysis between experimental average intensity data on product ions of CID-MS/SM spectra of cation at m/z 391.18 of sample ORB59709 (**Table 4**) and standard results from m^7G [96]: **(A)** linear relation between $D^{"}_{SD}$ data on Equation (2) of product ions at m/z 279, 167, and 149 of CID-MS/MS spectra of cation at m/z 391.18 of samples ORB59709 and ORB59710 (**Tables 4** and **S3**); **(B)** correlative analysis of $D^{"}_{SD}$ and D_{QC} data on Equations (2) and (3) of m^5U- and $m^1\Psi$-derivatives; **(C)** experimental CID-MS/MS spectrum of ion at m/z 243.10; **(D)** and chemical diagrams of species; **(E)** chemometrics.

4. Discussion

In this section, the discussion should focus on advantages of Equations (2) and (4) in determining nucleotides in mixtures as an attractive tool for MS-based structural analysis, comparing with routine approaches to process experimental variables. To develop the latter point there should be focused on issue of quantitative distinguishing between 3D molecular conformations and electronic structures of protomers,

tautomers, isomers, and rotamers of analytes exhibiting subtle electronic effects. It is an important theme, amongst others in application-oriented MS analysis of nucleotides. There has been argued elsewhere that in vivo exposure of DNA or RNA upon ionizing irradiation causes for their structural damage as most sensitive molecular targets in living systems. There is affected mainly on phosphate ester bond cleavage; thus, producing a set of chemical modifications of both nucleobases and CB-fragment. The modified molecules contribute to develop cancer. The research effort is concentrated on important task of structural analysis of nucleotides and their chemically modified derivatives in vivo. In doing so, the MS methods contribute crucially as irreplaceable approaches to identify molecules as result from their superior method performances and capability of in vivo assay and imaging techniques. However, frequently MS protocols fail to solve analytical problems for which they were intended. The structural analysis of nucleotide mixtures, their derivatives, and chemically modified analogues could be rather complicated determining structurally similar analytes; thus, highlighting species containing methyl and hydroxyl groups. Their stabilizing or destabilizing properties depend on macromolecular environmental factors. The uridine and thymidine derivatives are differ by both one OH- and CH_3-groups; thus, making difficult their separation. Further complication derives from presence of pseudouridine derivatives; if any. They show virtually identical MS fragmentation patterns, as well. The same is valid to derivatives of guanosine m^1G, m^2G, and m^7G isomers which are frequently assigned to mixture of analytes, mass spectrometrically. Given that, there is need to take seriously issue of capability of routine methods for data processing of MS variables. In analysing mixtures of nucleotides there has become part of problem of their reliable structural assignment due to low semi-quantitative performances of the methods, rather than to be tools for its solution. There is needed complementary employment in more precise approaches to process data on MS parameters allowing a reliable distinguishing of individual analyte among species having subtle variation of structural sub-units, including tackling subtle electronic effects of tautomers. Equations (2) and (4) overcome this drawback; thus, linking between the latter developed methodologically MS formulas and practical application oriented aspects of method for structural analysis of nucleotides. There is made crucial progress on discussed issue having significant prospective for broad interdisciplinary application to many research fields.

The discussion should start by explaining what there is understood under semi-quantitative determining of nucleotides and why there are assigned observable MS variables to mixtures of analytes instead of to individual molecules? Then, there shall be considered essential critique of routine approaches and how it relates known theories and practical application to mass spectrometry. Concluding statements shall reflect on implications of Equations (2) and (4) into MS-based structural analysis of nucleosides, their advantages, and contributions of current study to ongoing debates, regarding, capability of analytical mass spectrometry of reliable structural determining of individual analytes in biological samples, particularly concentrating the reader's attention on nucleosides.

Thus, an in-depth study of MS-based structural analysis of 1-methyl-, 2-methyl-, and 7-methyl-guanosine using standard samples of analytes [96] shows that linear correlation of intensity parameter of common peaks of derivatives m^1G and m^2G at

m/z 110, 128, 149, and 167 yields to $|r|$ = 0.91088, using routine approach to evaluate statistically average intensity data of peaks over whole time of measurements and data-base searching algorithms of mass spectra of standard samples. Particularly, complex is the structural analysis of mixtures of m^1G and m^7G showing correlation performances of intensity data on common peaks at m/z 110, 149, and 167 of $|r|$ = 0.99998; thus, lacking of reliable distinguishing of these species *via* classical tools. In the case of the studied in this paper samples tandem mass spectrometric results of intensity parameters of analytes and data on standards yield to $|r|$ = 0.9696. The obtained low performances and structural distinguishing among analytes *via* routine methods are not only due to significant fluctuations of measurands causing for large standard deviation, but also due to subtle variation of experimental intensity data lacking reliable determining of m^1G and m^7G derivatives. The same can be said for structural analysis of substituted pseudouridine showing product ions at m/z 125.03473, 155.04523, 179.04512, 209.05576, and 228.06889 [5] and produce $|r|$ = 0.07266–0.91257 comparing with standard sample. The data on this study reveals peaks at m/z 226.8, 208.91, 190.99, 178.93. 154.98, and 124.98 in agreement with work [32]. The classical analysis shows $|r|$ = 0.98053 correlating parameters with standard MS ones. Further: Mass spectrum of standard sample uridine reveals peaks at m/z 113.05, 96.008, 70.029, and 57.034, respectively. Its 5-methyl derivative m^5U is characterized by ions at m/z 127.057, 110.024, 84.044, 71.6, and 54.03 [96]. Correlative analysis between data on peaks of m^5U at m/z 127.05, 110.024, 84.044, 71.68, and 57.03 [96] and measurable variables of analytes in this study yields to $|r|$ = 0.34361–0.99718. Given that, there are semi-quantitative performances ($|r|$ = 0.99). Thus, any conclusion in structural assignment of discussed analytes based on only routine approaches should need to be tentative, rather than unambiguous one. There lies a question: How are we to carry out reliable theoretical sense of such cases; if any? Clearly, it is not explicitly explicable within the routine methods for data-processing of MS variables. There is needed novel concept in order to explain observable MS phenomena and the link between measurable parameters and molecular structure of analytes; furthermore, reliably and producing superior performances allowing to determine the discussed species in mixture unambiguously. The suggestion presented in this work is based on stochastic dynamics Equation (2) and its complementary employment in Arrhenius's Equation (3) allowing for tackling, on the one hand, fluctuations of variables per short span of scan time (Equation (2)). On the other hand, Equation (3) is capable of distinguishing between subtle electronic effects. It treats ionic vibrations of species in both ground and transition states. Perturbation of 3D molecular conformation and electronic structure of molecules affect sensitively their vibrational modes. Thus, chemometric assessment of relation $D"_{SD} = f(D_{QC})$ of parameters of Equation (2) and (3), in fact, assess link between MS intensity and its fluctuations as well as molecular and electronic structures of ions. A central task is to try to in-depth model and explain variations of intensity parameters of MS peaks within a large number of electronic effects of protomers, rotamers, and products of intramolecular rearrangement of ions; if any. The task excludes failure in trying to explain deeply electronic effects of nucleotides which vary broadly. Looking at results

from the current study it is empirically argued for claiming that there is achieved conclusive evidence of merits of presented approach showing $|r| = 0.99946$.

Therefore, it seems to me that implementation of innovative Equation (2) into MS based structural analysis of nucleotides even determining complex mixtures of derivatives of biological samples adds crucially not only to our further understanding of experimental MS phenomena, but also to increase in reliability of MS structural analysis of complex nucleotides exhibiting a diversity of electronic effects and isomers. The excellent performances achieved, herein, affect essentially on prospective application of the tool to many interdisciplinary research fields implementing routinely mass spectrometry for purposes of identification, annotation, and 3D structural analysis of nucleotides.

5. Conclusion

The innovative stochastic dynamics Equations (2) and (4) together with Arrhenius's Equation (3) through this study have proved to be significantly more effective and powerful tools for determining 3D structurally 5-methyluridine diphosphate N-acetylglucosamine containing m^5U structural sub-unit or N1-methyl-pseudouridine modified diphosphate in mixtures of nucleotides. These analytes produce virtually identical MS patterns and a set of common ions, particularly, highlighting low m/z-values. Due to the later fact, immediate difficulty arises when there is applied routine methods for data-processing of MS parameters of nucleotides which show semi-quantitative performances when there are compared analyte patterns with standard samples. The analysis of 5-methyl-uridine derivatives shows $|r| = 0.98831$. The difficulty of molecular structural analysis is mainly in specifying analyte tautomers, protomers, and rotamers together with their products of intramolecular rearrangement which can vary broadly. However, in the case of the stochastic dynamics method the 3D molecular and electronic structures of the analytes and fluctuations of experimental variables are handled exactly via Equations (2) and (3), thus, allowing for correlating reliably between observable parameters and molecular structures of analytes. As can be seen, there are achieved superior performances determining N1-methyl-pseudouridine modified diphosphate ($|r| = 0.9994–0.99923$). Conversely, analysis of proposed 5-methyluridine diphosphate N-acetylglucosamine shows $|r| = 0.98541–0.97402$. The obtained performances contrast significantly with those ones achieved via classical methods; thus, producing not only excellent coefficients of linear correlation between theory and experiment, but also it is significantly higher comparing with structurally similar derivative of 5-methyl-uridine producing virtually identical fragmentation patterns, particularly within m/z 600–0. The application to Equation (4) result in $|r| = 0.99459$. In parallel, performances of the innovative method are excellent comparing with classical methods yielding to semi-quantitative data, respectively, assignment of analytes, mass spectrometrically. The outcome of these data and observations is that Equations (2) and (4) show significant prospective application to mass spectrometric based structural analysis as powerful tool producing highly reliable quantitative and structural analysis of complex mixtures of nucleotides.

Supplementary materials: Chromatographic, mass spectrometric, theoretical quantum chemical data; and chemometrics (**Figures S1–S27** and **Tables S1–S7**.)

Acknowledgments: The author thanks the Deutsche Forschungsgemeinschaft; Alexander von Humboldt Stiftung; and Deutscher Akademischer Austausch Dienst for grants within various programs.

Conflict of interest: The author declares no conflict of interest.

References

1. Dávalos-Prado JZ, Megias-Perez R, Ros F, et al. Gas phase proton affinity and basicity of methylated uracil-derivatives. International Journal of Mass Spectrometry. 2021; 470: 116720. doi: 10.1016/j.ijms.2021.116720
2. Colasurdo DD, Pila MN, Iglesias DA, et al. Tautomerism of uracil and related compounds: A mass spectrometry study. European Journal of Mass Spectrometry. 2017; 24(2): 214-224. doi: 10.1177/1469066717712461
3. Barone V. DFT Meets Wave-Function Composite Methods for Characterizing Cytosine Tautomers in the Gas Phase. Journal of Chemical Theory and Computation. 2023; 19(15): 4970-4981. doi: 10.1021/acs.jctc.3c00465
4. Gosset-Erard C, Didierjean M, Pansanel J, et al. Nucleos'ID: A New Search Engine Enabling the Untargeted Identification of RNA Post-transcriptional Modifications from Tandem Mass Spectrometry Analyses of Nucleosides. Analytical Chemistry. 2023.
5. Ross RL, Yu N, Zhao R, et al. Automated Identification of Modified Nucleosides during HRAM-LC-MS/MS using a Metabolomics ID Workflow with Neutral Loss Detection. Journal of the American Society for Mass Spectrometry. 2023; 34(12): 2785-2792. doi: 10.1021/jasms.3c00298
6. Nakayama H, Yamauchi Y, Nobe Y, et al. Method for Direct Mass-Spectrometry-Based Identification of Monomethylated RNA Nucleoside Positional Isomers and Its Application to the Analysis of Leishmania rRNA. Analytical Chemistry. 2019; 91(24): 15634-15643. doi: 10.1021/acs.analchem.9b03735
7. Mi S, Cai S, Xue M, et al. HIF-1α/METTL1/m7G axis is involved in CRC response to hypoxia. Biochemical and Biophysical Research Communications. 2024; 693: 149385. doi: 10.1016/j.bbrc.2023.149385
8. Losito I, Angelico R, Introna B, et al. Cytosine to uracil conversion through hydrolytic deamination of cytidine monophosphate hydroxy-alkylated on the amino group: a liquid chromatography – electrospray ionization – mass spectrometry investigation. Journal of Mass Spectrometry. 2012; 47(10): 1384-1393. doi: 10.1002/jms.3078
9. Hayashi J, Hamada T, Sasaki I, et al. Synthesis of novel cationic spermine-conjugated phosphotriester oligonucleotide for improvement of cell membrane permeability. Bioorganic & Medicinal Chemistry Letters. 2015; 25(17): 3610-3615. doi: 10.1016/j.bmcl.2015.06.071
10. Ma B, Zarth AT, Carlson ES, et al. Methyl DNA Phosphate Adduct Formation in Rats Treated Chronically with 4-(Methylnitrosamino)-1-(3-pyridyl)-1-butanone and Enantiomers of Its Metabolite 4-(Methylnitrosamino)-1-(3-pyridyl)-1-butanol. Chemical Research in Toxicology. 2017; 31(1): 48-57. doi: 10.1021/acs.chemrestox.7b00281
11. Favretto D, Traldi P, Celon E, et al. Role of different 5-substituents on the mass spectrometric behaviour of uracil. Organic Mass Spectrometry. 1993; 28(10): 1179-1183. doi: 10.1002/oms.1210281032
12. Lönnberg T. Nucleic acids through condensation of nucleosides and phosphorous acid in the presence of sulfur. Beilstein Journal of Organic Chemistry. 2016; 12: 670-673. doi: 10.3762/bjoc.12.67
13. Guo S, Wang Y, Zhou D, et al. Electric Field-Assisted Matrix Coating Method Enhances the Detection of Small Molecule Metabolites for Mass Spectrometry Imaging. Analytical Chemistry. 2015; 87(12): 5860-5865. doi: 10.1021/ac504761t
14. Feliu C, Peyret H, Vautier D, et al. Simultaneous quantification of 8 nucleotides and adenosine in cells and their medium using UHPLC-HRMS. Journal of Chromatography B. 2020; 1148: 122156. doi: 10.1016/j.jchromb.2020.122156
15. Zhang Q, Liang J, Li X, et al. Exploring antithrombotic mechanisms and effective constituents of Lagopsis supina using an integrated strategy based on network pharmacology, molecular docking, metabolomics, and experimental verification in rats. Journal of Ethnopharmacology. 2025; 336: 118717. doi: 10.1016/j.jep.2024.118717
16. Brancato G, Rega N, Barone V. Microsolvation of uracil anion radical in aqueous solution: a QM/MM study. Chemical Physics Letters. 2010; 500(1-3): 104-110. doi: 10.1016/j.cplett.2010.09.078

17. Barannikov V, Tyunina E. Regularities of changes in thermodynamic parameters induced by the complex formation of uracil with some aromatic amio-acids in buffer solution and pH 7.4. ChemChemTech; 2022.
18. Nakajima K, Ito E, Ohtsubo K, et al. Mass Isotopomer Analysis of Metabolically Labeled Nucleotide Sugars and N- and O-Glycans for Tracing Nucleotide Sugar Metabolisms. Molecular & Cellular Proteomics. 2013; 12(9): 2468-2480. doi: 10.1074/mcp.m112.027151
19. Ito J, Herter T, Baidoo EEK, et al. Analysis of plant nucleotide sugars by hydrophilic interaction liquid chromatography and tandem mass spectrometry. Analytical Biochemistry. 2014; 448: 14-22. doi: 10.1016/j.ab.2013.11.026
20. Borisova M, Gisin J, Mayer C. The N-Acetylmuramic Acid 6-Phosphate Phosphatase MupP Completes the Pseudomonas Peptidoglycan Recycling Pathway Leading to Intrinsic Fosfomycin Resistance. mBio. 2017; 8(2). doi: 10.1128/mbio.00092-17
21. Konda S, Batchu UR, Nagendla NK, et al. Silver Nanoparticles Induced Metabolic Perturbations in Pseudomonas aeruginosa: Evaluation Using the UPLC-QTof-MSE Platform. Chemical Research in Toxicology. 2023; 37(1): 20-32. doi: 10.1021/acs.chemrestox.3c00154
22. Wang S, Zhang J, Wei F, et al. Facile Synthesis of Sugar Nucleotides from Common Sugars by the Cascade Conversion Strategy. Journal of the American Chemical Society. 2022; 144(22): 9980-9989. doi: 10.1021/jacs.2c03138
23. Liu H, Li Y, Du J, et al. Novel acetylation-aided migrating rearrangement of uridine-diphosphate-N-acetylglucosamine in electrospray ionization multistage tandem mass spectrometry. Journal of Mass Spectrometry. 2005; 41(2): 208-215. doi: 10.1002/jms.979
24. Fang J, Guan W, Cai L, et al. Systematic study on the broad nucleotide triphosphate specificity of the pyrophosphorylase domain of the N-acetylglucosamine-1-phosphate uridyltransferase from Escherichia coli K12. Bioorganic & Medicinal Chemistry Letters. 2009; 19(22): 6429-6432. doi: 10.1016/j.bmcl.2009.09.039
25. Jurga S, Barciszewski J. Epitranscriptomics. Springer International Publishing; 2021. doi: 10.1007/978-3-030-71612-7
26. Mosammaparast N. DNA Damage Responses. Springer US; 2022. doi: 10.1007/978-1-0716-2063-2
27. Jora M, Lobue PA, Ross RL, et al. Detection of ribonucleoside modifications by liquid chromatography coupled with mass spectrometry. Biochimica et Biophysica Acta (BBA) - Gene Regulatory Mechanisms. 2019; 1862(3): 280-290. doi: 10.1016/j.bbagrm.2018.10.012
28. Levola H, Kooser K, Itälä E, et al. Comparison of VUV radiation induced fragmentation of thymidine and uridine nucleosides—The effect of methyl and hydroxyl groups. International Journal of Mass Spectrometry. 2014; 370: 96-100. doi: 10.1016/j.ijms.2014.07.008
29. Wiebers JL, Shapiro JA. Sequence analysis of oligodeoxyribonucleotides by mass spectrometry. 1. Dinucleoside monophosphates. Biochemistry. 1977; 16(6): 1044-1050. doi: 10.1021/bi00625a003
30. Sugiyama C, Furusho A, Todoroki K, et al. Selective analysis of intracellular UDP-GlcNAc and UDP-GalNAc by hydrophilic interaction liquid chromatography-mass spectrometry. Analytical Methods. 2024; 16(12): 1821-1825. doi: 10.1039/d4ay00122b
31. Wilson MS, McCloskey JA. Chemical ionization mass spectrometry of nucleosides. Mechanisms of ion formation and estimations of proton affinity. Journal of the American Chemical Society. 1975; 97(12): 3436-3444. doi: 10.1021/ja00845a026
32. Dudley E, Bond L. Mass spectrometry analysis of nucleosides and nucleotides. Mass Spectrometry Reviews. 2013; 33(4): 302-331. doi: 10.1002/mas.21388
33. Wolken J, Turecek F. Proton affinity of uracil. A computational study of protonation sites. Journal of the American Society of Mass Spectrometry. 2000.
34. Abma GL, Parkes MA, Horke DA. Preparation of Tautomer-Pure Molecular Beams by Electrostatic Deflection. The Journal of Physical Chemistry Letters. 2024; 15(17): 4587-4592. doi: 10.1021/acs.jpclett.4c00768
35. Molina FL, Broquier M, Soorkia S, et al. Selective Tautomer Production and Cryogenic Ion Spectroscopy of Radical Cations: The Uracil and Thymine Cases. The Journal of Physical Chemistry A. 2024; 128(18): 3596-3603. doi: 10.1021/acs.jpca.4c02199
36. Salpin JY, Haldys V, Steinmetz V, et al. Protonation of methyluracils in the gas phase: The particular case of 3-methyluracil. International Journal of Mass Spectrometry. 2018; 429: 47-55. doi: 10.1016/j.ijms.2017.05.004

37. Nei Y, Akinyemi TE, Steill JD, et al. Infrared multiple photon dissociation action spectroscopy of protonated uracil and thiouracils: Effects of thioketo-substitution on gas-phase conformation. International Journal of Mass Spectrometry. 2010; 297(1-3): 139-151. doi: 10.1016/j.ijms.2010.08.005
38. Ryszka M, Pandey R, Rizk C, et al. Dissociative multi-photon ionization of isolated uracil and uracil-adenine complexes. International Journal of Mass Spectrometry. 2016; 396: 48-54. doi: 10.1016/j.ijms.2015.12.006
39. Mirzoyan VS, Melik-Ogandzhanyan RG, Rusavskaya TN, et al. Investigation of azoles and azines. 76. Mass spectra of 5- and 6-substituted uracils. Chemistry of Heterocyclic Compounds. 1990; 26(4): 446-455. doi: 10.1007/bf00497220
40. Ivanova B, Spiteller M. An Experimental and Theoretical Mass Spectrometric Quantification of Non-Covalent Interactions in High Order Homogeneous Self-Associates of Nucleobases and Nucleosides. NOVA Science Publisher; 2018.
41. Razakov R, Kasimov AK. Study of nucleic acid bases by the DADI method. Chemistry of Natural Compounds. 1979; 15(6): 743-747. doi: 10.1007/bf00565577
42. Chen W, Liu Y, Wei M, et al. Studies on effect of Ginkgo biloba L. leaves in acute gout with hyperuricemia model rats by using UPLC-ESI-Q-TOF/MS metabolomic approach. RSC Advances. 2017; 7(68): 42964-42972. doi: 10.1039/c7ra08519b
43. Chen C, Laviolette SR, Whitehead SN, et al. Imaging of Neurotransmitters and Small Molecules in Brain Tissues Using Laser Desorption/Ionization Mass Spectrometry Assisted with Zinc Oxide Nanoparticles. Journal of the American Society for Mass Spectrometry. 2021; 32(4): 1065-1079. doi: 10.1021/jasms.1c00021
44. Wu J, McLuckey SA. Gas-phase fragmentation of oligonucleotide ions. International Journal of Mass Spectrometry. 2004; 237(2-3): 197-241. doi: 10.1016/j.ijms.2004.06.014
45. Zeng J, Wang Z, Huang X, et al. Comprehensive Profiling by Non-targeted Stable Isotope Tracing Capillary Electrophoresis-Mass Spectrometry: A New Tool Complementing Metabolomic Analyses of Polar Metabolites. Chemistry–A European Journal. 2019; 25(21): 5427-5432. doi: 10.1002/chem.201900539
46. Moseley HN, Lane AN, Belshoff AC, et al. A novel deconvolution method for modeling UDP-N-acetyl-D-glucosamine biosynthetic pathways based on 13C mass isotopologue profiles under non-steady-state conditions. BMC Biology. 2011; 9(1). doi: 10.1186/1741-7007-9-37
47. Garcia AD, Chavez JL, Mechref Y. Sugar nucleotide quantification using multiple reaction monitoring liquid chromatography/tandem mass spectrometry. Rapid Communications in Mass Spectrometry. 2013; 27(15): 1794-1800. doi: 10.1002/rcm.6631
48. Antoniewicz MR. A guide to 13C metabolic flux analysis for the cancer biologist. Experimental & Molecular Medicine. 2018; 50(4): 1-13. doi: 10.1038/s12276-018-0060-y
49. Wang Z, Liu PK, Li L. A Tutorial Review of Labeling Methods in Mass Spectrometry-Based Quantitative Proteomics. ACS Measurement Science Au. 2024; 4(4): 315-337. doi: 10.1021/acsmeasuresciau.4c00007
50. Duan L, Cooper DE, Scheidemantle G, et al. 13C tracer analysis suggests extensive recycling of endogenous CO2 in vivo. Cancer & Metabolism. 2022; 10(1). doi: 10.1186/s40170-022-00287-8
51. Bowman MJ, Zaia J. Tags for the Stable Isotopic Labeling of Carbohydrates and Quantitative Analysis by Mass Spectrometry. Analytical Chemistry. 2007; 79(15): 5777-5784. doi: 10.1021/ac070581b
52. Cooks RG, Kruger TL. Intrinsic basicity determination using metastable ions. Journal of the American Chemical Society. 1977; 99(4): 1279-1281. doi: 10.1021/ja00446a059
53. McLuckey SA, Cameron D, Cooks RG. Proton affinities from dissociations of proton-bound dimers. Journal of the American Chemical Society. 1981; 103(6): 1313-1317. doi: 10.1021/ja00396a001
54. Kenttaemaa H, Cooks R. Internal energy distribution acquired through collision activation at low and high energies. International Journal of Mass Spectrometry. 1985.
55. Collette C, De Pauw E. Calibration of the internal energy distribution of ions produced by electrospray. Rapid Comminication in Mass. Spectrometry; 1988.
56. Kertesz TM, Hall LH, Hill DW, et al. CE50: Quantifying collision induced dissociation energy for small molecule characterization and identification. Journal of the American Society for Mass Spectrometry. 2009; 20(9): 1759-1767. doi: 10.1016/j.jasms.2009.06.002
57. Carlo MJ, Nanney ALM, Patrick AL. Energy-Resolved In-Source Collison-Induced Dissociation for Isomer Discrimination. Journal of the American Society for Mass Spectrometry. 2024; 35(11): 2631-2641. doi: 10.1021/jasms.4c00118

58. Jankowski W, Hoffmann M, Półrul P, et al. Study of protonated dimers of cytosine, cytidine, and deoxycytidine using survival yield method and quantum mechanics calculations. Rapid Communications in Mass Spectrometry. 2023; 37(24). doi: 10.1002/rcm.9661
59. Meng C, Han Q, Wang X, et al. Determination and Quantitative Comparison of Nucleosides in two Cordyceps by HPLC–ESI–MS-MS. Journal of Chromatographic Science. 2019; 57(5): 426-433. doi: 10.1093/chromsci/bmz012
60. Li Z, Zhang HX, Li Y, et al. Method for Quantification of Ribonucleotides and Deoxyribonucleotides in Human Cells Using (Trimethylsilyl) diazomethane Derivatization Followed by Liquid Chromatography–Tandem Mass Spectrometry. Analytical Chemistry. 2018; 91(1): 1019-1026. doi: 10.1021/acs.analchem.8b04281
61. Strzelecka D, Chmielinski S, Bednarek S, et al. Analysis of mononucleotides by tandem mass spectrometry: investigation of fragmentation pathways for phosphate- and ribose-modified nucleotide analogues. Scientific Reports. 2017; 7(1). doi: 10.1038/s41598-017-09416-6
62. Soo EC, Aubry AJ, Logan SM, et al. Selective Detection and Identification of Sugar Nucleotides by CE−Electrospray-MS and Its Application to Bacterial Metabolomics. Analytical Chemistry. 2003; 76(3): 619-626. doi: 10.1021/ac034875i
63. Addepalli B, Limbach PA. Mass Spectrometry-Based Quantification of Pseudouridine in RNA. Journal of the American Society for Mass Spectrometry. 2011; 22(8): 1363-1372. doi: 10.1007/s13361-011-0137-5
64. Cherneva TD, Todorova MM, Bakalska RI, et al. Experimental and theoretical study of the cytosine tautomerism through excited states. Journal of Molecular Modeling. 2023; 29(10). doi: 10.1007/s00894-023-05707-0
65. Wang WJ, Wang T, Zhao Y, et al. Theoretical Insights into N-Glycoside Bond Cleavage of 5-Carboxycytosine by Thymine DNA Glycosylase: A QM/MM Study. The Journal of Physical Chemistry B. 2024; 128(19): 4621-4630. doi: 10.1021/acs.jpcb.4c00221
66. Parida C, Chowdhuri S. Solvation structure and hydrogen bond dynamics of uracil–water and thymine–water: A comparison of different force fields of uracil and thymine. Chemical Physics Letters. 2024; 846: 141357. doi: 10.1016/j.cplett.2024.141357
67. Ivanova B. Stochastic Dynamic Mass Spectrometric Quantitative and Structural Analyses of Pharmaceutics and Biocides in Biota and Sewage Sludge. International Journal of Molecular Sciences. 2023; 24(7): 6306. doi: 10.3390/ijms24076306
68. Ivanova B. Structural Analysis of Polylactic Acid in Composite Starch Biopolymers—A Stochastic Dynamics Mass Spectrometric Approach. Innovation Discovery. 2024; 1(3): 26. doi: 10.53964/id.2024026
69. Ivanova B. Stochastic dynamics mass spectrometric and Fourier transform infrared spectroscopic structural analyses of composite biodegradable plastics. Pollution Study. 2024; 5(1): 2741. doi: 10.54517/ps.v5i1.2741
70. Ivanova B. Stochastic dynamics mass spectrometric structural analysis of poly(methyl methacrylate). Universal Journal of Carbon Research. 2024.
71. Ivanova B, Spiteller M. Stochastic Dynamic Electrospray Ionization Mass Spectrometric Quantitative Analysis of Metronidazole in Human Urine. Analytical Chemistry Letters. 2022; 12(3): 322-348. doi: 10.1080/22297928.2022.2086822
72. Borges AL, Thuy-Boun P. Orbitrap LC-MS/MS data for phage nucleosides(1.0) [Data set]. Zenodo; 2022. doi: 10.5281/ZENODO.7319990.
73. Frisch M, Trucks G, Schlegel H, et al. Gaussian 09, 98. Gaussian, Inc., Pittsburgh, Wallingford CT; 2009.
74. Helgaker T, Jensen H, Jrgensen P, et al. Dalton Program Package. [https://daltonprogram.org/]; 2011.
75. Gordon MS, Schmidt MW. Advances in electronic structure theory. Theory and Applications of Computational Chemistry; Elsevier, Amsterdam, 2005.
76. Nielsen A, Holder A. Gauss View 5.0, User's Reference. Pittsburgh GausView03 Program Package. GAUSSIAN Inc.; 2009.
77. Burkert U, Allinger N. Molecular mechanics in ACS Monograph 177. American Chemical Society, Washington D.C.; 1982.
78. Allinger NL. Conformational analysis. 130. MM2. A hydrocarbon force field utilizing V1 and V2 torsional terms. Journal of the American Chemical Society. 1977; 99(25): 8127-8134. doi: 10.1021/ja00467a001
79. Hempel A, Lane BG, Camerman N. Pseudouridine. Acta Crystallographica Section C Crystal Structure Communications. 1997; 53(11): 1707-1709. doi: 10.1107/s0108270197009323
80. Kelley C. Iterative Methods for optimization. SIAM Front. Appl. Mathematics; 2009.
81. Otto M. Chemometrics, 3rd ed. Wiley, Weinheim; 2017.
82. Apache OpenOffice. Available online: http://de.openoffice.org (accessed on 3 May 2024).
83. Madsen K, Nielsen H, Tingleff T. Informatics and mathematical modelling, 2nd ed. DTU Press; 2004.
84. Miller J, Miller J. Statistics and chemometrics for analytical chemistry. Pentice Hall, London; 1988.

85. Taylor J. Quality assurance of chemical measurements. Lewis Publishers, Inc; 1987.
86. Schroee G, Trenkler D. Exact and randomization distributions of Kolmogorov-Smirnov tests two or three samples. Computational Statistics & Data Analysis; 1995.
87. Fay MP, Proschan MA. Wilcoxon-Mann-Whitney or t-test? On assumptions for hypothesis tests and multiple interpretations of decision rules. Statistics Surveys. 2010; 4(none). doi: 10.1214/09-ss051
88. Freidlin B, Gastwirth JL. Should the Median Test be Retired from General Use? The American Statistician. 2000; 54(3): 161-164. doi: 10.1080/00031305.2000.10474539
89. Li Y, Yu H, Zhao W, et al. Analysis of urinary methylated nucleosides of patients with coronary artery disease by high-performance liquid chromatography/electrospray ionization tandem mass spectrometry. Rapid Communications in Mass Spectrometry. 2014; 28(19): 2054-2058. doi: 10.1002/rcm.6986
90. Thumbs P. Synthese der natürlichen tRNA-Modifikation Galaktosylqueuosin und Untersuchungen zur Struktur der natürlichen tRNA-Modifikation Mannosylqueuosin. LMU Munich; 2013.
91. Thumbs P, Ensfelder TT, Hillmeier M, et al. Synthesis of Galactosyl-Queuosine and Distribution of Hypermodified Q-Nucleosides in Mouse Tissues. Angewandte Chemie International Edition. 2020; 59(30): 12352-12356. doi: 10.1002/anie.202002295
92. Pichler A, Hillmeier M, Heiss M, et al. Synthesis and Structure Elucidation of Glutamyl-Queuosine. Journal of the American Chemical Society. 2023; 145(47): 25528-25532. doi: 10.1021/jacs.3c10075
93. Shaw SJ, Desiderio DM, Tsuboyama K, et al. Mass spectrometry of nucleic acid components. Analogs of adenosine. Journal of the American Chemical Society. 1970; 92(8): 2510-2522. doi: 10.1021/ja00711a049
94. Muftakhov MV, Shchukin PV. Resonant electron capture by uridine and deoxyuridine molecules: Fragmentation with charge transfer. Rapid Communications in Mass Spectrometry. 2019; 33(5): 482-490. doi: 10.1002/rcm.8354
95. Ptasińska S, Candori P, Denifl S, et al. Dissociative ionization of the nucleosides thymidine and uridine by electron impact. Chemical Physics Letters. 2005; 409(4-6): 270-276. doi: 10.1016/j.cplett.2005.04.102
96. Jora M, Burns AP, Ross RL, et al. Differentiating Positional Isomers of Nucleoside Modifications by Higher-Energy Collisional Dissociation Mass Spectrometry (HCD MS). Journal of the American Society for Mass Spectrometry. 2018; 29(8): 1745-1756. doi: 10.1007/s13361-018-1999-6
97. Giessing AMB, Scott LG, Kirpekar F. A Nano-Chip-LC/MSn Based Strategy for Characterization of Modified Nucleosides Using Reduced Porous Graphitic Carbon as a Stationary Phase. Journal of the American Society for Mass Spectrometry. 2011; 22(7). doi: 10.1007/s13361-011-0126-8
98. Habermehl G, Christ BG. Synthese von Pseudouridin C. Justus Liebigs Annalen der Chemie. 1978; 1978(3): 427-430. doi: 10.1002/jlac.197819780308
99. Ji M, Lee H, Kim Y, et al. Metabolomic Study of Normal and Modified Nucleosides in the Urine of Mice with Lipopolysaccharide-Induced Sepsis by LC–MS/MS. Bulletin of the Korean Chemical Society. 2021; 42(4): 611-617. doi: 10.1002/bkcs.12240
100. Wei F, Yuan R, Wen Q, et al. Systematic Enzymatic Synthesis of dTDP-Activated Sugar Nucleotides. Angewandte Chemie International Edition. 2023; 62(20). doi: 10.1002/anie.202217894
101. Fang J, Xue M, Gu G, et al. A chemoenzymatic route to synthesize unnatural sugar nucleotides using a novel N-acetylglucosamine-1-phosphate pyrophosphorylase from Camphylobacter jejuni NCTC 11168. Bioorganic & Medicinal Chemistry Letters. 2013; 23(15): 4303-4307. doi: 10.1016/j.bmcl.2013.06.003
102. Guo Z, Li J, Qin H, et al. Biosynthesis of the Carbamoylated D-Gulosamine Moiety of Streptothricins: Involvement of a Guanidino-N-glycosyltransferase and an N-Acetyl-D-gulosamine Deacetylase. Angewandte Chemie International Edition. 2015; 54(17): 5175-5178. doi: 10.1002/anie.201412190
103. Li S, Wang S, Wang Y, et al. Gram-scale production of sugar nucleotides and their derivatives. Green Chemistry. 2021; 23(7): 2628-2633. doi: 10.1039/d1gc00711d
104. Masuko S, Bera S, Green DE, et al. Chemoenzymatic Synthesis of Uridine Diphosphate-GlcNAc and Uridine Diphosphate-GalNAc Analogs for the Preparation of Unnatural Glycosaminoglycans. The Journal of Organic Chemistry. 2012; 77(3): 1449-1456. doi: 10.1021/jo202322k
105. McLuckey S, Van Berkel G, Glish G. Tandem mass spectrometry of small, multiply charged oligonucleotides. Journal of the American Society for Mass Spectrometry. 1992.

106. Hogg AM, Kelland JG, Vederas JC, et al. Nucleosides and nucleotides part 24 Investigation of ribo- and deoxyribonucleosides and -nucleotides by fast- atom-bombardment mass spectrometry. Helvetica Chimica Acta. 1986; 69(4): 908-917. doi: 10.1002/hlca.19860690419
107. Price NPJ, Jackson MA, Vermillion KE, et al. Rhodium-catalyzed reductive modification of pyrimidine nucleosides, nucleotide phosphates, and sugar nucleotides. Carbohydrate Research. 2020; 488: 107893. doi: 10.1016/j.carres.2019.107893
108. Haas TM, Mundinger S, Qiu D, et al. Stable Isotope Phosphate Labelling of Diverse Metabolites is Enabled by a Family of 18O-Phosphoramidites**. Angewandte Chemie International Edition. 2021; 61(5). doi: 10.1002/anie.202112457
109. Kammerer B, Frickenschmidt A, Müller CE, et al. Mass spectrometric identification of modified urinary nucleosides used as potential biomedical markers by LC–ITMS coupling. Analytical and Bioanalytical Chemistry. 2005; 382(4): 1017-1026. doi: 10.1007/s00216-005-3232-2
110. Luan T, Su G, He Y, et al. Isolation and Identification of Water-Soluble Nitrogenous Compounds of Chlorella Growth Factors from Chlorella pyrenoidosa. Chemistry of Natural Compounds. 2024; 60(3): 592-594. doi: 10.1007/s10600-024-04390-8
111. Liu C, Dou X, Zhao Y, et al. IGF2BP3 promotes mRNA degradation through internal m7G modification. Nature Communications. 2024; 15(1). doi: 10.1038/s41467-024-51634-w
112. Unger SE, Schoen AE, Cooks RG, et al. Identification of modified nucleosides by secondary-ion and laser-desorption mass spectrometry. The Journal of Organic Chemistry. 1981; 46(23): 4765-4769. doi: 10.1021/jo00336a028
113. Tuytten R, Lemière F, Esmans EL, et al. In-source CID of guanosine: Gas phase ion-molecule reactions. Journal of the American Society for Mass Spectrometry. 2006; 17(8): 1050-1062. doi: 10.1016/j.jasms.2006.03.012
114. Kasprzyk R, Starek BJ, Ciechanowicz S, et al. Fluorescent Turn-On Probes for the Development of Binding and Hydrolytic Activity Assays for mRNA Cap-Recognizing Proteins. Chemistry—A European Journal. 2019; 25(27): 6728-6740. doi: 10.1002/chem.201900051
115. Strenkowska M, Wanat P, Ziemniak M, et al. Preparation of Synthetically Challenging Nucleotides Using Cyanoethyl P-Imidazolides and Microwaves. Organic Letters. 2012; 14(18): 4782-4785. doi: 10.1021/ol302071f
116. Raczyńska ED, Zientara K, Kolczyńska K, et al. Change of tautomeric equilibria, intramolecular interactions and π-electron delocalization when going from phenol to uracil. Journal of Molecular Structure: THEOCHEM. 2009; 894(1-3): 103-111. doi: 10.1016/j.theochem.2008.10.025
117. Raczyńska ED, Zientara K, Stępniewski TM, et al. Stability, polarity, intramolecular interactions and π-electron delocalization for all eighteen tautomers rotamers of uracil. DFT studies in the gas phase. Collection of Czechoslovak Chemical Communications. 2009; 74(1): 57-72. doi: 10.1135/cccc2008149
118. Udagawa T. Theoretical analysis on the aromaticity of uracil: Important electronic configurations and solvent effect on the aromaticity. Chemical Physics Letters. 2015; 637: 115-119. doi: 10.1016/j.cplett.2015.07.057
119. Roberts JD, Streitwieser A, Regan CM. Small-Ring Compounds. X. Molecular Orbital Calculations of Properties of Some Small-Ring Hydrocarbons and Free Radicals1. Journal of the American Chemical Society. 1952; 74(18): 4579-4582. doi: 10.1021/ja01138a038
120. Dewar M. The molecular orbital theory of organic chemistry. McGraw-Hill, New York, 1969.
121. Burrows CJ, Muller JG. Oxidative Nucleobase Modifications Leading to Strand Scission. Chemical Reviews. 1998; 98(3): 1109-1152. doi: 10.1021/cr960421s
122. Vemula H, Bobba S, Putty S, et al. Ion-pairing liquid chromatography–tandem mass spectrometry-based quantification of uridine diphosphate-linked intermediates in the Staphylococcus aureus cell wall biosynthesis pathway. Analytical Biochemistry. 2014; 465: 12-19. doi: 10.1016/j.ab.2014.07.024
123. Chandran J, Aravind U, Aravindakumar C. Sonochemical transformation of thymidine: A mass spectrometric study. Ultrasonics Sonochemistry. 2015; 27.